ANALYTICAL TOOL FOR MODELING THE CYCLIC BEHAVIOUR OF EXTENDED END-PLATE CONNECTIONS

Author: Mohd Fazaulnizam Bin Shamsudin

Supervisor: Professor Carlos A. Silva Rebelo

University: University of Coimbra

University: University of Coimbra

Date: 13.01.2014

ACKNOWLEDGEMENTS

I would like to express my sincere appreciation and gratitude to the supervisor of this thesis, Prof. Carlos Rebelo for guiding me in doing this work. His valuable advices, suggestions, patience and comments are highly appreciated. I am highly indebted to his for his valuable thoughts and contributions towards the development of my thesis and also for providing me with an ample knowledge about seismic design.

Special thanks are also extended to my colleague, Hugo Augusto who is supporting me throughout the course of this research. His generosity and always there to help me will not be forgotten. Also, his invaluable suggestions and constructive comments encouraged me too numerous to count.

The help of Prof. Luís Simões da Silva who is one of the SUSCOS programme coordinator really in way to help me in completing this project. I wish to take this opportunity to forward my utmost appreciation to all the lecturers in the Department of Civil Engineering in Coimbra University, Czech Technical University and all of friends in this programme for their contributions throughout my study in the university. I was very fortunate to share part of the journey in my life particularly in Europe with these incredible people.

Dedicating this dissertation to my family for their endless love, support and encouragement over the past years. Huge thanks for understanding my passion and interest to push myself beyond the limit. Finally, deepest gratefulness to God for He always directs my path to conquer the quests to success in this momentary life.

RESUMO

Neste trabalho é apresentada uma investigação computacional sobre estudar o modelo de histerese e o comportamento cíclico de ligação viga-pilar . O modelo da ligação estudada e os resultados do comportamento cíclico correspondem aos obtidos em testes experimentais descritos na bibliografia. Foi utilizado o software SeismoStruct para modelar a ligação e foi desenvolvida uma folha de cálculo para gerar as curvas de histerese diretamente a partir do Modelo Modificado de Richard- Abbott com trinta parâmetros. Foi usado o protocolo ECCS para gerar as historias de carga. Os parâmetros do modelo foram alterados para observar a sensibilidade em termos de resistência, rigidez e capacidade de dissipação de energia. Os resultados experimentais e computacionais relativos às curvas de histerese momento-rotação foram comparados com os resultados do modelo analítico implementado nume folha de cálculo.

ABSTRACT

A computational investigation was conducted to study the hysteretic model and cyclic behaviour of beam to column connection. The connection model was taken from experimental test setup and data was used in the software SeismoStruct and in numerical tool spreadsheet to perform the hysteretic curves. The beam to column joints were analysed according to Modified Richard-Abbott Model with thirty model parameters particularly well determined for cyclic loads which covered lower and upper bound curves. ECCS cyclic loading protocol which correlates with displacements as a common practice was used to generate time-history load curves. The model parameters were altered and applied on the joint to observe the sensitivity of parameters in term of strength, stiffness and energy dissipation capacity. Experimental and computational results of moment-rotation curves were compared with analytical approach. The sensitivity of the results to certain coefficients was studied to measure the differences of resulted value and numerical implementation in order to detect errors and achieve the same result.

TABLE OF CONTENTS

LIST OF FIGURES

LIST OF TABLES

SYMBOLS

Ka – Ascending Initial Stiffness

Ma – Descending Strength

Kpa – Ascending Post Limit Stiffness

Kd – Descending Initial Stiffness

Md – Descending Strength

Kpd – Descending Post Limit Stiffness

iMa – Strength Damage Rate

ABBREVIATIONS

EC3 – Eurocode 1993-1-1:2005

MRF – Moment Resisting Frame

HSFG – High Strength Friction Grip

AISC – American Institute of Steel Construction

MATLAB – Matrix Laboratory

FEM – Finite Element Method

HSS – Hollow Structural Sections

ECCS – European Convention for Constructional Steelwork

CHAPTER I: INTRODUCTION AND LITERATURE REVIEW

1.1 Introduction

In the beam-column connections, bolted steel connections in the form of T-stubs and end-plate connections are designed as assemblages of components such as bolts, plates, and welds. Because of the possibility in several variety of connection joint configurations, many geometrical discontinuities and associated stress concentrations triggered on bolted connections in beam to column structure. Also, presence of frictional forces that lead to non-linear phenomena such as slip and the need to model uplift and contact forces that can lead to prying action, then these connections exhibit an overall nonlinear structural behaviour commonly classified as "semi-rigid".

Eurocode 3 [1] contains design rules for determining the properties of several types of connections including the bolted flush end-plate. Beam-to-column joints are often subjected to a combination of bending and axial forces. Part 1-8 of Eurocode 3 [1] classifies joints by their stiffness (nominally pinned, rigid or semi-rigid), or by their strength (nominally pinned, full-strength or partial-strength). In relation to stiffness, a nominally pinned joint will allow rotation, transmitting forces across the joint without developing significant moments. A rigid joint, however, is stiff enough for the analysis to be based on full continuity, and a semi-rigid joint lies between these two. In terms of strength, a nominally pinned joint is defined as for stiffness while a full-strength joint has a moment resistance greater than that of the connected members. The partial-strength joint does develop moment, but the moment resistance is less than that of the connected members. It is especially advantageous for partial-strength and semi-rigid joints to develop sufficient rotation capacity before loss of moment resistance.

Various researches on the behaviour and design of steel connections under seismic loads have been conducted over the past several years. Although moment resisting frames (MRF) are commonly used structural system for seismic-resistant buildings, several important aspects of their behaviour under real earthquake excitation are not well understood. One of these issues that need to be further studied is the seismic performance of beam to column joints. During severe earthquakes, joints can undergo severe inelastic deformations affecting the strength, stiffness and inelastic action distribution throughout the frames.

For seismic design purposes, fully welded connections are traditionally used in moment resisting frames. More economical types of bolted connections were not utilized mainly due to their relative flexibility and difficulty to achieve full resistance as compared to fully welded forms, which may lead to large deformations under the same forces. Whereas this treatment applies for static conditions, the response under dynamic loading may be substantially different. Due to the period elongation of the frame as well as the higher energy dissipation in the connection, semi-rigid frames may attract lower loads and possess higher damping. Consequently, the displacements associated with bolted frames may be lower than that experienced in their welded counterparts. (A. S. Elnashai, 1998)

Recently pertaining on seismic design concept levels of structural response, behaviour and safety are applied. The general and fundamental idea is that small to medium level of earthquakes should not cause significant damages in the structure. However, the collapse under extreme earthquakes should be avoided and certain structural damages are acceptable. Practically, the structure should be able to sustain elastic actions under smaller case and inelastic response while sustain severe seismic actions. In addition, an inelastic response should be controlled in order to prevent structural collapse.

1.2 Previous Research on Hysteretic Model with the Cyclic Response of Steel Joints

P. Nogueiro, L. Simões da Silva, R. Bento (2003) analysed an influence of joint slippage on the cyclic response of steel frames. The purpose of this paper is to discuss the various hysteretic models available to model steel joints under cyclic loading, describing a numerical models implementation with and without slippage, comparing distinct joints under cyclic response with and without slippage as well as assessing the structure on global behaviour impetus by influence of slippage. The Richard-Abbott model which is based on a formula in 1975 was used to reproduce the elastic-plastic behaviour of several materials and was initially used to simulate the static monotonic response of joints and then applied to cyclic response. The modified model proposed by Mazzolani (De Martino et al., 1984; Mazzolani, 1988), which is based on the Ramberg-Osgood model also used which allows the simulation of hysteretic curves with slippage. On the numerical implementation and experimental calibration, it was observed that the controlling variable is rotation, φ for the Richard-Abbott model and bending moment, M for the modified Mazzolani model. It is noted that the edge beam-column connection exhibits more significant slippage while continuous beam barely shows pinching effect. Based on the case study of typical of a low-rise office building, the response and influence of joint slippage and degradation on the cyclic behaviour of steel frames was presented in this paper. They concluded that because of the unavailability of a joint element with degradation and slippage in the global analysis, an indirect approach was used, using an equivalent bi-linear spring.

Pedro Nogueiro, Luís Simões da Silva, Rita Bento and Rui Simões (2006) conducted a series of experimental tests to determine the hysteretic model with pinching. The cyclic response of generic steel joints were implemented in computer with an adaptation of the model in a spring element within SeismoStruct. Extended end-plate connection tests were performed to investigate the influence of the loading history on the joint performance as well as setting the key parameters which enabling a full description of connection behaviour including energy dissipation capability. The tests were incorporated in software SeismoStruct and showing a very good agreement with the experimental results, even when using different loading strategies. They concluded that 15 parameters in ascending and 15 parameters in descending are the same. The parameters that results from static monotonic behaviour (Ka, Ma, Kpa, Kd, Md, Kpd) can nowadays be obtained with sufficient accuracy from the application of the component method (EC3-1-8, 2005) for the range of joint typologies addressed in this paper. For joints without pinching and stiffness deterioration, such as an extended end-plate with stiffened column web in the tensile and compressive areas, only 6 parameters are needed. From these parameters, the first three can be obtained using the component method and the fourth is normally 1 or 2. The last one it is always the same, equal to 0.1 rad. Finally, the

parameter related to the strength damage (iMa), can be established as an average value on the basis of a sufficient number of tests.

G. Della Corte, G. De Matteis, R. Landolfo, F.M. Mazzolani (2001) performed experiments regarding seismic analysis of moment-resisting (MR) steel frames based on refined hysteretic models of connections. The analyses presented in this paper show that safety margins against global collapse of the structure can be predicted only by considering more realistic hysteresis behaviour, i.e. using mathematical models able to take account of strength degradation and pinching phenomena. Moreover, it is shown that the design of conventional steel building systems according to the European seismic code may lead to over-resistant structures, due to the limitation on inter-storey drift angles for non-structural damage control under frequent earthquakes. It is also noticed that this result is inevitable, owing to the indications provided by Eurocode 8 in terms of both prescribed inter-storey drift limits and assumed base shear-force demand under frequent earthquakes.

Several numerical analyses have been carried out and results shown throughout the current paper. Two main conclusions can be drawn:

i) The elastic-perfectly-plastic hysteresis model is adequate in obtaining a reliable prediction of deformation demand for (EC8) code-designed structures, and for seismic intensities less than or equal to the one stipulated by the code for the ultimate limit state check. In the relevant deformation range, variability of deformation demand due to ground motion is largely dominant in comparison to that related to the hysteresis model. However, safety at collapse for the frame as a whole (dynamic instability) can only be predicted by adopting more refined hysteresis models, able to take account of degradation phenomena.

ii) Design of steel structures according to EC8 leads to strongly over-resistant structures, due to the limitation on inter-storey drift angles under frequent earthquakes (serviceability requirement). When judging the effect of degradation phenomena on the seismic performance of steel moment resisting frames, this over-strengthening should be taken into account, since it reduces the impact of degradation itself.

L. Mota, A. T. da Silva, C. Rebelo, L. Simões da Silva and L. de Lima (2010) expanded the knowledge of modelling connections of moment resisting steel frames with the implementation of seismic analysis. The modified Richard-Abbott constitutes a sophisticated model and is used here to reproduce the cyclic behaviour of the steel joints. The main goal in this paper was to determine the influence of stiffness degradation, strength degradation and hardening effect of the joint under seismic behaviour of a three storey two bays moment

resisting (MR) steel frame. They concluded that the maximum global displacements increases for higher hardening effect and decreases for higher stiffness degradation and strength degradation. The reason because for moment resisting frames the horizontal displacement is usually the controlling design criterion in seismic design. On the other hand, that maximum rotation in links is not very sensitive to stiffness degradation and strength degradation.

Cavidan YORGUN (2001) developed an evaluation of innovative extended end-plate moment connections under cyclic loading. The comparison between standard end-plate connections and innovative end endplate connections was performed using experimental results and design methods. There was no deformation in the I-shaped element placed between the end plate and the column flange and it remained elastic. Hysteretic loops for specimens exhibited stable characteristics, but the specimens did not develop the same level ductility ratios. The primary purpose of the testing process was to investigate the influence of end-plate thickness and gap (filled in with I-shaped element, i.e. beam section) and to check this against design criteria developed for monotonic loading. Predicted capacities obtained using the component method coded in Eurocode 3 were compared to data obtained experimentally. The maximum moment strengths of the connections were much greater than the strength predictions from the design method of Eurocode 3. Finally, the design method used to predict connection strength was shown to be conservative when compared with the experimental strength for the innovative end-plate connections.

Mohsen Geramia, Hamid Saberia, Vahid Saberia and Amir Saedi Daryan (2010) presented the findings of cyclic behaviour of bolted connections with different arrangement of bolts. Following the discovery of earthquakes failures, numerous experimental and analytical investigations were initiated to obtain a moment connection that will provide the required combination of strength, stiffness, and ductility while resisting cracking. Therefore, various types of connections such as end plate and T-stub bolted connections were suggested to be used in design of moment resisting frames in areas of high seismic activity. In this study, the cyclic behaviour of end plate and T-stub beam-to-column bolted connections is analysed and compared for different arrangements of bolts using finite element analysis. The results of numerical models showed a good agreement with the test data. One of the finding is the probability of failure mode change in T-stub connection is higher than that of end plate connection under cyclic loading due to the bolt arrangement change. Therefore, the end plate connection is suggested for conditions where the imperfection in construction is probable.

Shemy S. Babu, S. Sreekumar (2012) conducted a study on the ductility of bolted beam-column connections**.** In this paper the ductility and energy dissipation characteristics of semi rigid bolted connections using double web angle with top and seat angles is discussed based on experimental investigation. Non-linear analysis was also performed using finite element

method to compare the results. The study revealed that ductile behaviour of beam-column connection is improved by increasing the number of bolts on the top and seat angles and the thickness of top and seat angles. The analytical results are in agreement with the experimental results. Based on the experimental and analytical investigation conducted on bolted steel beam-column joint, the following conclusions are drawn:

i) The use of top and seat angles improved the energy dissipation capacity. The energy dissipation of the connection increases as the thickness of top and seat angles and number of bolts increases.

ii) Increasing the number of bolts rather than increasing the diameter of bolt in the connection with top and bottom seat angles improves ductility.

S.Aleksić and S.R. Živaljević (2008) presented a paper describing analysis of the dynamic response of steel orthogonal frames with non-linear semi-rigid connections under the seismic loads. Chen-Lui exponential curve was used for the mathematical modelling of the non-linear beam-column connections. Direct integration of the equations of motion was performed with the so-called α-procedure. The general numerical procedure was programmed in MATLAB and used for numerical example presented in this paper. This paper is based on the usage of the capacity design method in seismic designing. Namely, with the nonlinear behaviour of the connections beam-column, the seismic forces are limited in the structure, in that way the members of the structure are kept in the desirable (usually linear) range, while the largest part of the seismic energy is spent in the hysteresis behaviour of the connections. In this way, nonlinear beam-column connections present some kind of safety devices, consciously designed bad points in the structure, which, including the necessary rotation capacity, make the structure to move like a mechanism in limited case, during the formation of the plastic hinges in the frame fixity, and while the elements of the complex structure are in the desirable (linear) range of stresses. The conclusion is that the relation of the dynamic characteristics of the structure in respect to the dynamic characteristics of the seismic loads has a key role during the analysis of the seismic resistance of the structure.

Satish Kumar and Prasada Rao D. V. (2004) conducted a study in seismic qualification of semi-rigid connections in steel frames. The results of cyclic test conducted on a semi-rigid connection with rectangular hollow sections, consists of channel connectors welded to the column and connected to the beam by HSFG bolts installed through a web opening were presented. Several requirements were identified for semi-rigid connections to qualify for use in seismic resisting frames. The tested connections were found to have adequate stiffness, ultimate strength, ductility and energy dissipation capacity as per the requirements.

John C. Ryan, Jr. (1999) conducted a research regarding the evaluation of extended end-plate moment connections under seismic loading**.** In this paper, an experimental investigation was conducted to study the extended end-plate moment connections subjected to cyclic loading. The connections were designed using yield-line theory to predict end-plate yielding and the modified Kennedy method to predict maximum bolt force calculations including prying action. The inelastic rotation of connections was calculated and conclusions were drawn on the compliance of these connections with current AISC specifications. They concluded that all extended stiffened moment end-plate configurations demonstrated the ability to incur sufficient inelastic rotation to be used in a moment frame designed for seismic loading. As a result of observing the weld failures of these connections, it is recommended that full-penetration welds be used for beam to end-plate welds, beam-to-stiffener welds and stiffener-to-end-plate welds. Finally, the design methods used to predict connection strength are shown to be conservative when compared with the experimental strengths for the four bolt extended stiffened moment end-plate connections.

Mark R. Boorse (1999) performed experiments on evaluation of the inelastic rotation capability of flush end-plate moment connections. An experimental investigation also was conducted to study the inelastic rotation capability of flush end-plate moment connections. Experimental results for maximum moment resisted by the connections were compared with analytical predictions. Moment strengths of the connections were calculated using yield-line theory to predict end-plate yielding and maximum bolt force calculations including prying action. Experimental results were also compared to previous research with regards to strength and stiffness. It was found that the connections with a wide connection allowed for more yielding of the end-plate during testing. These connections exhibited nearly double the inelastic rotation capability than their tight counterparts.

1.3 End-Plate Beam to Column Connections

End-plate moment connections consist of a plate that is shop-welded to the end of a beam that is then field bolted to the connecting member using rows of high strength bolts. The connections are primarily used to connect a beam to a column or to splice two beams together. Bolted end-plate connections are extensively used for connecting beams to columns or beams to beams in multi-storey steel frame buildings. There are several types of end-plate connections: extended end-plate, as shown in Figure 1.1 and flush end-plate, as shown in Figure 1.2. For seismic design purposes, rigid connections are traditionally used in moment resisting frames. Steel frames with semi-rigid connections were not utilized mainly due to their relative flexibility when compared to rigid forms.

The extended end-plate connection is primarily used for beam-to-column connections. It consists of a plate with bolt holes drilled or punched, and shop welded to a beam section. The connection is completed in the field when the beam end is bolted to a column. The extended end-plate connection is termed “extended” because the plate extends above or below the flange that will be in tension under load. In the case of extended end-plates used for seismic design, the end-plate is extended above and below both beam flanges. Extended end-plate connections can be stiffened or unstiffened. The stiffened configurations have gusset plate (stiffener) welded to the outside of the beam flange, as shown in Figure 1.1. The stiffener is aligned with the web of the connecting beam to strengthen the extended portion of the end-plate. This type of connections can be used in frames subjected to both vertical loads and horizontal forces due to wind action or seismic motion. In general, bolted extended end-plate connections are able to dissipate significant amounts of energy, and are suitable for seismic-resistant structures (Ghobarah et al., 1992). The four-bolt, stiffened and unstiffened extended end-plate design procedures were concluded to be sufficient for cyclic loading, and therefore for use in steel buildings subject to seismic activity (John C. Ryan, 1999).

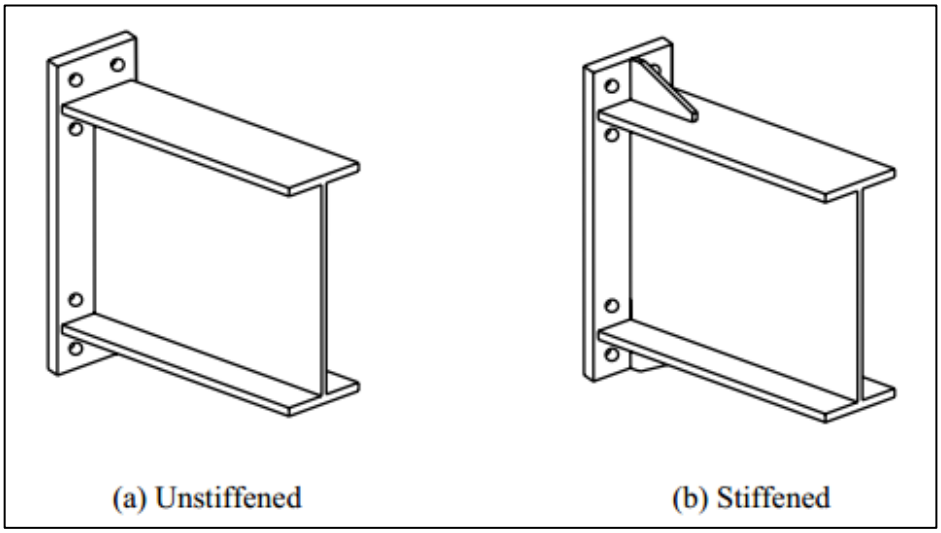

Figure 1.1 Examples of Extended End-Plate Connection

The beam-to-column flush end-plate connection consists of a steel plate welded to the end of an I-beam. The end-plate is then bolted to the column flange using various rows of fully tensioned high-strength bolts. The flush end-plate moment connection is one in which the end-plate does not extend above the beam flange. One or two rows of bolts at each flange can be used. Flush end-plate connections can be stiffened or unstiffened. The stiffened configurations have gusset plates (stiffeners) welded to the beam and to the end-plate on both sides of the web. Figure 1.2 shows the four-bolt flush with and without stiffened configurations.

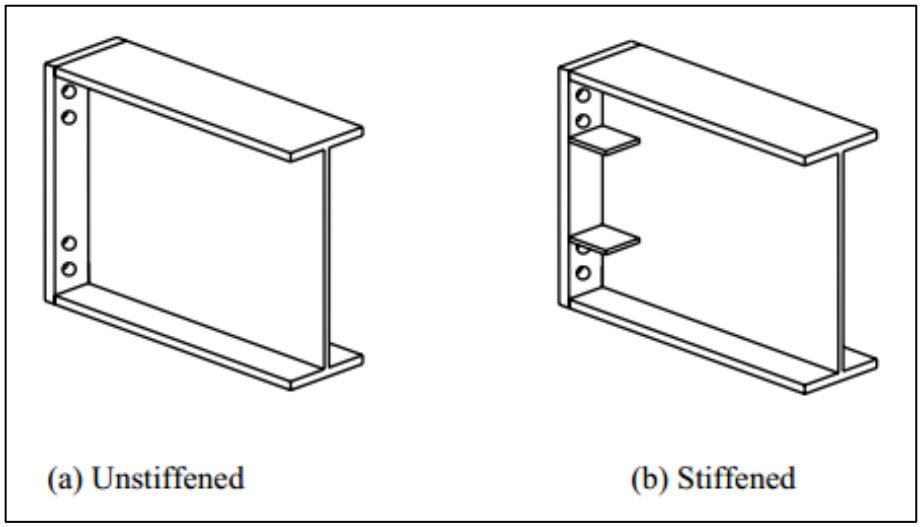

Figure 1.2 Examples of Flush End-Plate Connection

Moment end-plate connections are further described by the number of bolts at the tension flange and the configuration of the bolt rows. For gravity and or wind load applications, the end plate connection is often designed to carry tension only at one flange. For seismic or cyclic loading, where the connection may experience load reversals, the end-plate is designed to carry tension at both flanges.

The primary advantage of moment end-plate connections is that they do not require field welding, allowing to be done in cold conditions, and construction time to be reduced. They are easy to build and cost approximately the same as other moment connections. They allow a great variety of structural solutions by properly modifying the connection structural detail. In particular, both rotational stiffness and flexural resistance can be properly balanced by choosing an appropriate number of bolts and their location, an appropriate end-plate thickness and its geometrical configuration. The primary disadvantages are that they require precise beam length and bolt holes location tolerances.

This method of construction offers several advantages over other joint types (Griffifths, 1984 and Murray, 1988):

i) The joint is suitable for winter erection, since only field bolting is required.

ii) All welding is performed in the shop thus eliminating any field welding associated problems and offering high quality control.

iii) The number of bolts required for erection purposes is relatively small compared to other fully bolted joints, which makes the erection process relatively fast and efficient.

The most important structural properties of the joints that should be known prior to the analysis of frame structure and the design of its members are the moment resistance, rotational stiffness, and rotation capacity.

1.4 Component Method

1.4.1 Introduction

The application of component method to connection modelling design needs three basic steps. Firstly, identification of the components of the joints, secondly, evaluation of force-deflection diagram of independent components and finally the components are assembled imposing compatibility equations to determine strength, stiffness and deformation capacity of the entire connection. Previously connections were designed as either pinned or fixed full strength connection. The accuracy of the component method depends on the accuracy quality of the components assembling process. Moreover, certain mechanical components do not behave independently being related to others. The application of the component method is capable to analyse different types of connection topologies. Contrarily to previous design code the procedures to design according to component method are complex requiring considerable effort even when designing a simple moment connection. Software has been developed to determine mechanical properties especially under monotonic loading. Generally, the loading is assumed to be imposed on the structure in two different ways as shown in Figure 1.3 (Ádány S., 2000). Monotonic loading means the classical static loading having the following characteristics:

i) quasi-static,

ii) Its intensity is increasing in time.

While cyclic loading represents a simplified seismic loading with the features as follows:

i) quasi-static,

ii) repeated loading-unloading-reversed loading-unloading,

iii) Its intensity is high enough to cause significant plastic strain in the structure.

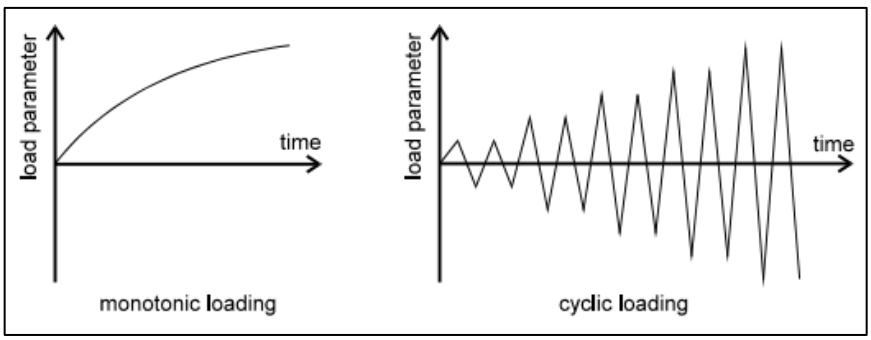

Figure 1.3 Monotonic and cyclic loading

1.4.2 Static Loading

1.4.2.1 Characteristics Behaviour of Connection Parameters

i) **Column web panel in shear (ductile):** The limitation of the column web slenderness satisfies the condition $d_c / t_w \leq 69\varepsilon$ is there to ensure that no shear buckling occurs. As $\varepsilon = \sqrt{235 / f_{ywc}}$ (with f_{ywc} = yield stress of the column web in N / mm^2), the steel grade is already taken into consideration there and no other limitation is required; in other words, the formula given in Annex J for the plastic shear resistance of the panel is valid whatever the steel grade, as long as $d_c / t_w \leq 69\varepsilon$. The limitation to S355 can therefore be removed.

ii) **Column web in compression (fragile):** The only component for which an extending of the design rules to HSS seems quite questionable is the column web in compression where the buckling and crippling resistances (not the crushing one) are highly dependent on the web slenderness and the longitudinal stresses in the column web resulting from bending moments and normal forces.

iii) **Beam flange and web in compression (ductile):** The strength evaluation is based on the evaluation of the design resistance $M_{c,Rd}$ of the beam section. $M_{c,Rd}$ is dependent on the class of the beam profile and, as for the column web in shear, this one is influenced by ε. A priority, no limitation of the steel grades seems to be needed for this component, but the validation of the related design formula for strength would anyway be welcome. The additional web welds were intended to increase the amount of bending moment transferred by the web connection, thereby relieving somewhat the moment transferred by the flange welds (Engelhardt and Husain 1993). Regarding beam flange and web in compression, local buckling phenomenon can result in a dissipative behaviour provided that the width-to-thickness ratios of the plate elements constituting the beam section are limited to assure a ductile behaviour, i.e., class 1 cross-sections are adopted.

iv) **End plate in bending, Column flange in bending and Flange cleat in bending:** These components are idealized as T-stubs subjected to tension forces. At design collapse, the bolts fail in tension, a plastic mechanism develops in the T-stub flange or a mixed failure involving bolt fracture and plasticity in the T-stub flange occurs. Once again, the relative values of the yield stresses (bolts/plate) are taken

into consideration in the strength calculations and no limitation of the yield stress for the connected plate (end plate, column flange or cleat) has to be considered for these components. Moreover, the cyclic behaviour of bolted connections can be strongly affected by bolt plastic deformation, because the occurrence of such plastic deformations can lead to pinching phenomena of hysteresis loops of bolted components, i.e., endplate, column flange, and flange cleat in bending.

v) **Bolts in bearing, Plate in tension and compression, Beam web in tension, Column web in tension:** No instability is likely to occur in these components, even for the plate in compression, where the risk of instability is prevented through the use of appropriate bolt pitches. Their strength is linked to plasticity and a limitation to steel grade lower then S355 does not appear as quite justified. Regarding bolt behaviour, it is important to note that, both under normal and shear stresses, their limited plastic deformation capacity and fatigue life can lead to the brittle collapse of the joint, so that bolts have to be designed with sufficient over strength to prevent brittle failure modes.

1.4.2.2 Design Moment-Rotation Characteristic

As explained and indicated from the previous section, the main properties required for the analysis of a connection the moment resistance $M_{j,Rd}$, rotational stiffness S_j and the rotational capacity ϕ_{Cd} . Figure 1.3 gives an example of influence of joints beam-column connection and force directions. The moment resistance model orientation is shown in Figure 1.4. The corresponding moment (force) – rotation (displacement) curves are non-linear which typical feature of joint behaviour. The joint behaviour could be in rigid under torsion or shear, in semi-rigid influenced bending or axial force.

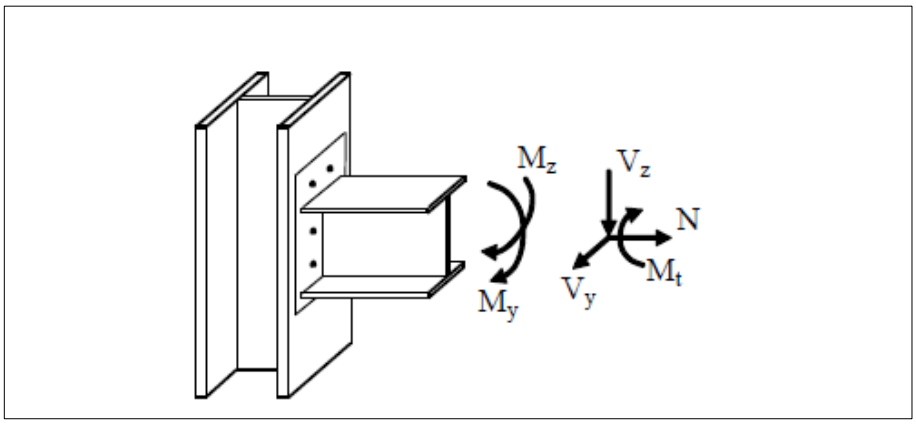

Figure 1.4 Influence of Bolted End-Plate Steel Joints

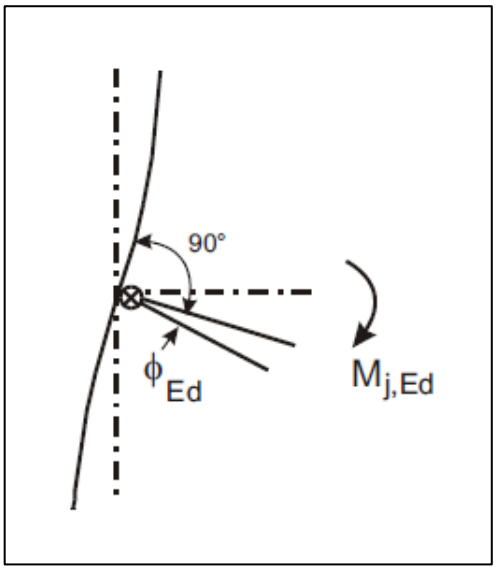

Figure 1.5 Model Orientation of Moment Resistance

The linear elastic curve deviates from its low bending moment straight line as shown in Figure 1.6. Moment-rotation curve presents initially an elastic behaviour, followed by a plastic response resulting from the progressive yielding of some components. After reaching 2/3 of the bending moment rotation curve, the component stiffness is reduced until the moment is reached. The required rotational capacity of a joint is depend on the structural type either statically determined or statically indeterminate and the analysis for the entire structure either in elastic or plastic behaviour. EC-1-8 defines such an equivalent elastic stiffness as expressed in equation 1.1.

$$S_j = \frac{S_{j,ini}}{\eta} \tag{1.1}$$

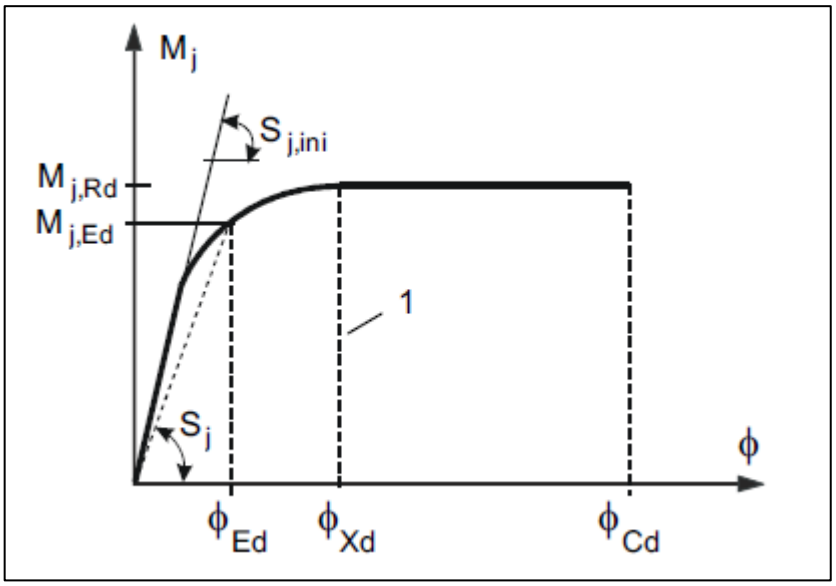

Figure 1.6 Design Moment Rotation Curve

In the calculation of the deformation capacity, it is important to consider possibility of unfavourable differences between the numerical strength and the actual strength. The column flange and the end plate in bending and the column web panel in shear are ductile joint components. The bolts in tension and shear and welds are typical examples of brittle components. Thus, both types mode of failure should not bother the strength of the connection.

1.4.3 Cyclic Loading

1.4.3.1 Loading Protocols

i) **Requirements of EN 15129:** The basic test protocol specified in EN 15129 is shown in Figure 1.7. The standard protocol states that the number of test cycles at the design displacement level shall be increased for devices with fundamental periods considerably less than 2s. For structures equipped with buckling restrained braced frame (BRBF) generally have a fundamental period in between 1-2s, therefore an appropriate load increment of test cycles is necessary.

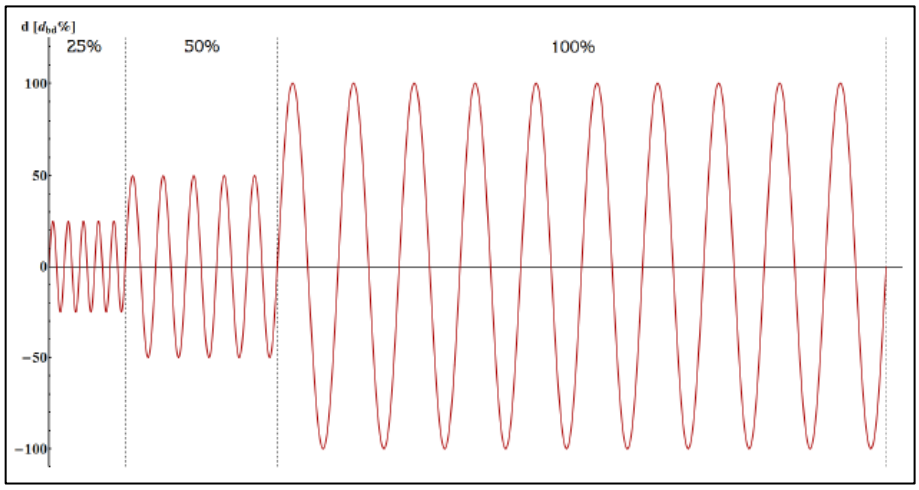

Figure 1.7 Loading Protocol specified in EN 15129

ii) **Load Protocol Proposed by ECCS:** Loading protocol provided by the European Convention for Constructional Steelwork (ECCS) for carry out tests in order to characterize the structural behaviour of structural components under cyclic loads as implemented in this paper. ECCS loading protocol apply different approach from EN 15129 protocol, the amplitude of load cycles is depending on the yield displacement (ey, identical to dy) in this case as shown in Figure 1.7. The third testing procedure provided by ECCS is a cyclic test with increase of displacement. The characteristics are defined as follows:

- One cycle in the $e_y^+ / 4 , e_y^- / 4$ interval;
- One cycle in the $2e_y^+ / 4 , 2e_y^- / 4$ interval;
- One cycle in the $3e_y^+ / 4 , 3e_y^- / 4$ interval;
- One cycle in the e_y^+ , e_y^- interval;
- Three cycles in the $2e_y^+ , 2e_y^-$ interval;
- Three cycles in the $(2+2n)e_y^+ , (2+2n)e_y^-$ interval (n=1,2,...).

More cycles or more intervals may be used if necessary. Displacements at yield are defined as:

$$e_y^+ = \frac{F_y^+}{tg a_y^+}$$

$$e_y^- = \frac{F_y^-}{tg a_y^-}$$

Where:

$F_y^{+/-}$ is the yield load in the positive/negative force range

$tg a_y^{+/-}$ is the slope of the tangent at the origin of the (F-e) curve, when F increases on the positive/negative side.

Yield displacement is estimated using characteristic material properties before the tests and verified after first yield during every experiment.

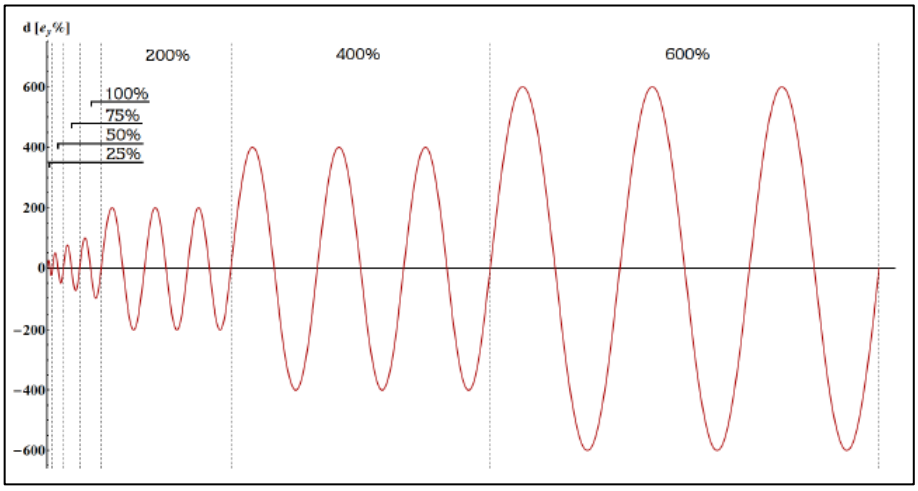

Figure 1.8 Loading Protocol specified in ECCS

iii) **SAC Loading protocol:** The basic SAC loading protocol is the multiple step tests in which the loading deformation history consists of stepwise increasing deformation cycles. The loading protocol based on displacement and is illustrated in Figure 1.9 and in tabular form as shown in Table 1.1. The cycles shall be symmetric in peak deformations. The history is devoted into several steps and the peak deformation of each step j is given as θj, a predetermined value of the inter-story drift angle. Thus, the loading history is defined by the following parameters:

θj the peak deformation in load step j

nj the number of cycles to be performed in load step j

Table 1.1 SAC Loading protocol

Load Step #	Peak Deformation, θ	Number of Cycles, n
1	0.00375	6
2	0.005	6
3	0.0075	6
4	0.01	4
5	0.015	2
6	0.02	2
7	0.03	2
Continue wih increments in θ of 0.01 rad, and perform two cycles at each step		

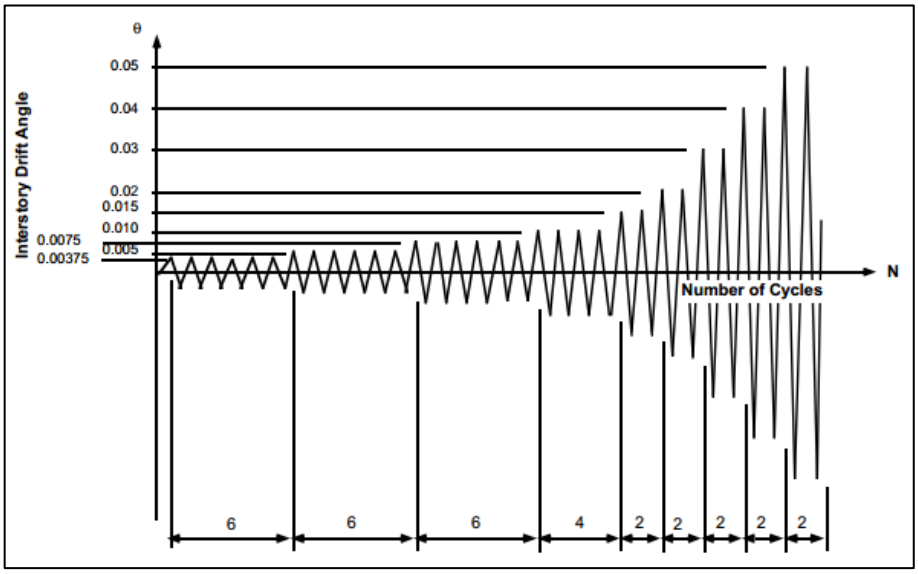

Figure 1.9 SAC Loading Protocol

iv) ATC-24 Loading protocol

Loading protocol provided by ATC-24 as shown in Figure 1.10 recommended several numbers of cycles and peak deformations in each load step as follows:

a) The number of cycles n_o with a peak deformation less than δ_y should be at least six.

b) The number of cycles n_1 with a peak deformation δ_y equal to δ_1 should be at least three.

c) The number of cycles n_2 with peak deformation $\delta_2 = \delta_y + \Delta$ should be at least three unless a lower number can be justified.

d) The number of cycles n_3 with peak deformation $\delta_3 = \delta_y + 2\Delta$ should be at least three.

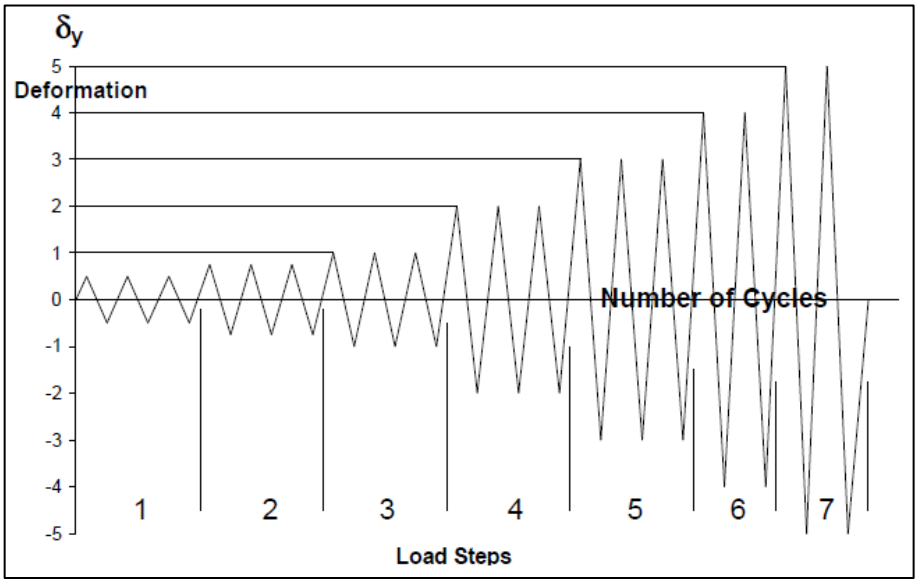

Figure 1.10 ATC-24 Loading Protocol

1.5 Objective and Scope

To address the need for an understanding of the cyclic behaviour and thereafter propose an appropriate cyclic model parameters for beam to column connections. An analysis software SeismoStruct and numerical study based on Richard-Abbott Model was conducted. The computational part consisted of two phases. The first involved investigating the cyclic behaviour of extended end-plate joints. The scope of the software SeismoStruct in this phase consisted of the following aspects:

i) Assessing the cyclic performance of end-plate beam to column connections.

ii) Examining the behaviour of the individual thirty cyclic model parameters comprising the connection such as the end-plate, the column flange and the bolts.

iii) Recommending design model parameters for joint under cyclic loading excitation to perform satisfactorily dissipative moment joint which related to pinching.

iv) The accuracy of it would need to be verified by comparing such results with relevant information from experimental tests.

In the second phase of the numerical approach that take into account the strength degradation and pinching phenomena were investigated by the implementation of Spreadsheet analysis. The results of rotation were taken from analytical analysis output and applied into the formulation of Modified Richard-Abbott model. The scope of the analytical analysis in this phase consisted of the following:

i) Checking the validity of the model parameters design criteria adopted from SeismoStruct and compared with resulted moment-rotation hysteretic curves generated by Spreadsheet.

ii) Improving the percentage of errors in bending moment with alteration of certain coefficient in Modified Richard-Abbott model.

iii) Developing the analytical model capable of predicting the behaviour of the beam-column connection.

iv) The performance of this model would be assessed by comparing the numerical hysteretic curves with the SeismoStruct results.

Chapter II: DOUBLE EXTENDED END-PLATE CONNECTION

2.1 Introduction

The behaviour of the beam-column connection plays a major role in the response of a steel moment resisting framed structure subjected to seismic loading excitation. Semi-rigid connections like bolted joints, are common type of connections and can be used to allow better energy dissipation in moment resisting frames (MRF) or in dissipative parts of braced frames. In this chapter the ductility and energy dissipation characteristics of semi-rigid bolted connections using double extended end-plate as shown in Figure 2.1 (Nogueiro, P., 2009) is discussed based on computational analysis.

In the steel structural framework with semi-rigid connections, the component characteristics of joints play a vital role in dissipating energy mechanisms. Rigid connections are costly and difficult to assemble and use of semi-rigid connections is justified. Semi-rigid connections connecting the web and flanges of the beam to the column flange are cheaper and simpler to assemble when compared to other conservative joint.

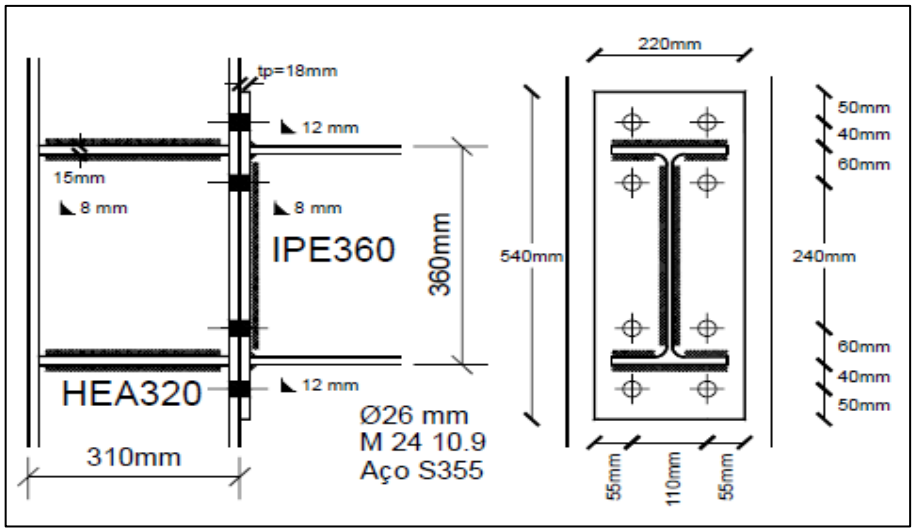

Figure 2.1 Double Extended End-Plate Connection Topology

2.2 Modified Richard-Abbott Model

The Richard-Abbott model is based on a formula developed in 1975 [Richard et al., 1975] to reproduce the elastic-plastic behaviour of several materials and was initially used to simulate the static monotonic response of joints and later applied to cyclic situations. According to this model, the loading branch of the moment-rotation curve of a joint is described by equation (1).

$$M = \frac{\left(k - k_p\right).\phi}{\left[1 + \left|\frac{\left(k - k_p\right).\phi}{M_o}\right|^N\right]^{1/N}} - k_p.\phi \tag{1}$$

Where M denotes the bending moment and ϕ the joint rotation. Parameters k, k_p and M_0 are defined in Figure 2.2, while N may be related with these parameters by the following equation:

$$N = \frac{-\ln 2}{\ln\left(\frac{M_1}{M_0} - \frac{k_p}{k - k_p}\right)} \tag{2}$$

In asymmetrical joints with respect to the centroidal axis, as in the case of composite joints, the model must be modified in accordance with Figure 2.2. The loading curve for a generic branch is now given by the equation (3).

$$M = M_n - \frac{\left(k_a - k_{pa}\right).\left(\phi_n - \phi\right)}{\left[1 + \left|\frac{\left(k_a - k_{pa}\right).\left(\phi_n - \phi\right)}{M_{oa}}\right|^N\right]^{1/N}} - k_{pa}.\left(\phi_n - \phi\right) \tag{3}$$

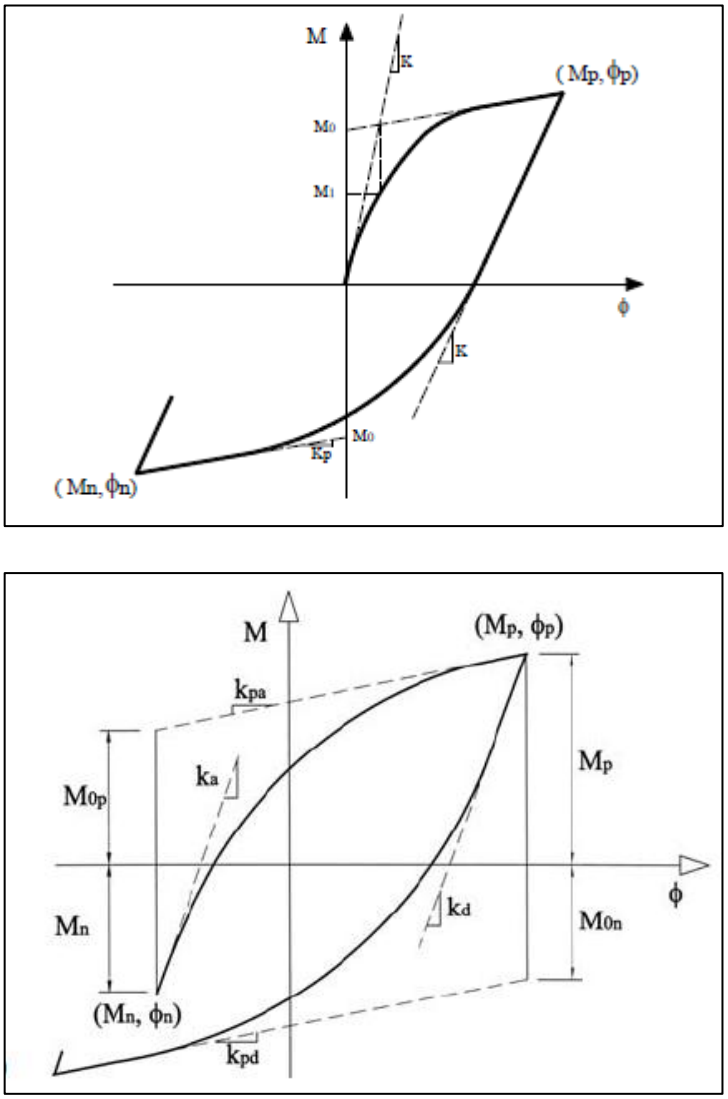

Figure 2.2 Richard-Abbott Model for Lower and Upper Bound

2.3 Cyclic Modeling of Dissipative and Non- Dissipative Components

2.3.1 Introduction

The capacity of design should control an inelastic behaviour. Based on the fundamental philosophy of design capacity, plastic deformations should be concentrated in pre-defined locations of the structure while the rest of the structure should remain in the elastic range. The application on seismic design should consider cyclic behaviour of structural components as follows (Ádány S., 2000):

i) The zones of the structure where extensive plastic deformations are expected, the so-called dissipative zones, have the major role of dissipating, by their inelastic hysteresis behaviour, the input energy coming from the ground motion in case of a severe earthquake. Thus, first of all, the dissipative zones should have enough energy absorption capacity.

ii) Moreover, it is essential for the dissipative zones to have enough ductility to allow the extensive structural deflections without failure, as well as to make possible the development of plastic hysteresis cycles that are necessary for the energy dissipation.

iii) At the same time it is important to know the strength (capacity) of the dissipative zones, by taking into consideration the effect of possible material hardening, in order to be able to design the connecting non-dissipative part of the structure to provide with resistance enough to remain in the elastic domain. (Note that the name of capacity design comes from the fact that non-dissipative zones should be designed for the actions equal to the capacity of the neighbouring dissipative zones.)

iv) Finally, it is important to know the rigidity change of the dissipative zones, since the dramatic rigidity degradation in several locations can lead to the development of global collapse mechanism of the structure that cannot be allowed.

2.3.2 Column Web Panel

Column web panel is defined as the column web component restricted by the continuity of the beam plates and the column flanges in any position of beam-column connections respectively. This area component is studied to be a zone primarily subjected to shear stresses behaviour and thereby its failure mode is controlled by shear yielding as shown in Figure 2.3. Previous research demonstrated that the mode of failure was stable and ductile. Thus, allowed the column web panel dissipate more energy under cyclic loading. These attractive characteristics were taken into account in design rules by the late of the 1980's which permitted the panel zone component to be counted as a dissipative component.

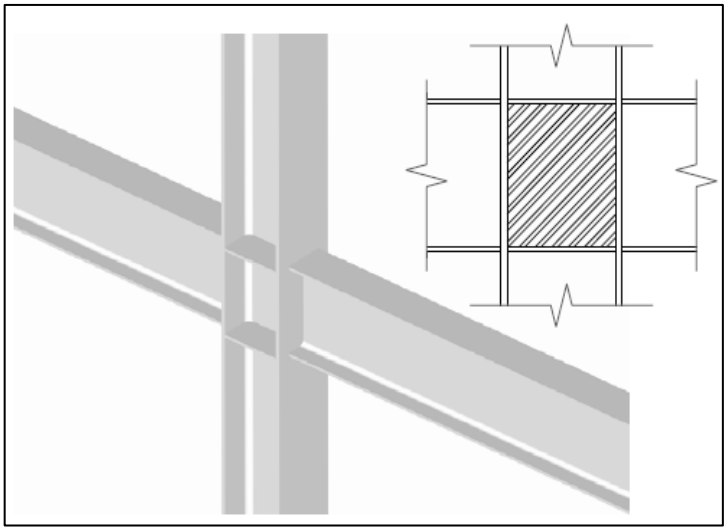

Figure 2.3 Panel Zone

The ductility performance of the panel zone was strengthened in Europe by Dubina et al. [2001] and Ciutina and Dubina [2006] in the research of understanding the cyclic performance of beam-column connections. Research documented ductility component triggering the capability of dissipating energy or even more by allowing stable hysteretic loops.

Based on previous study, the theoretical analysis of the yield condition of the web panel were conducted and validated versus experimental tests. The common load behaviour from the web panel was characterised by three stages. First, elastic shear response followed by yielding, according to the Von Mises criterion. Second, reserve in strength attributed to the surrounding elements of the panel. Finally, a post yield strength characterised by strain hardening of the steel. The post yield range was considered to be stable and to sustain considerable load after

the yield capacity. The panel was recognized as dissipating energy component. Considerations of the elastic and inelastic range of the web panel was determined by experimental and detail analytical understanding of the load deformation behaviour of joints and the associated strain-stress regime.

Column web in compression is well known that do not usually allow the development of highly dissipative mechanics under local buckling phenomena. For this reason, the use of stiffeners such as continuity plates is commonly suggested in designing the column web panel. In addition, doubler plates were sometimes provided in the column to increase the column panel zone shear strength. Column stiffeners can be designed to prevent local flange bending, local web yielding, local web crippling, and compression buckling of the column. Stiffeners are placed on the column at the locations of the beam flange forces to prevent distortion of the column flange where the beam exerts the tensile loading and web yielding and crippling at the compression loading. The beam is therefore exerting a tensile force through one flange and a compressive force through the other as shown in Figure 2.4.

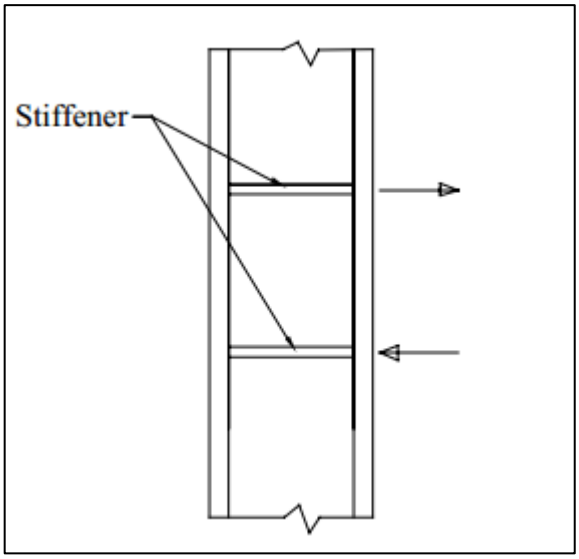

Figure 2.4 Couple Moment Transfer

In the application of cyclic behaviour, experimental tests were carried out by Nogueiro et al [6] and shown stable hysteretic loops with little strength and degradation and no pinching provided. The Table 2.1 shows the Modified Richard-Abbott model parameters determined

from Eurocode provisions and previous experimental tests and Table 2.2 below lists model parameters used to compute the moment-rotation hysteretic curve in the SeismoStruct.

Table 2.1 Model Parameters for Column Web Panel in Shear

$K_a = K_d = K_{ap} = K_{dp}$ (KNm/rad)	EC3-1-8
$M_a = M_d = M_{ap} = M_{dp}$ (KNm)	EC3-1-8
$K_{pa} = K_{pd} = K_{pap} = K_{pdp}$ (KNm/rad)	[1]
$n_a = n_d = n_{ap} = n_{dp}$	1
$t_{1a} = t_{2a} = t_{1d} = t_{2d} = C_a = C_d$	0
$i_{Ka} = i_{Kd}$	0
$i_{Ma} = i_{Md}$	0
$H_a = H_d$	0

Table 2.2 Example of Model Parameters for Column Web Panel in Shear

$K_a = K_d = K_{ap} = K_{dp}$ (KNm/rad)	35000
$M_a = M_d = M_{ap} = M_{dp}$ (KNm)	120
$K_{pa} = K_{pd} = K_{pap} = K_{pdp}$ (KNm/rad)	1000
$n_a = n_d = n_{ap} = n_{dp}$	1
$t_{1a} = t_{2a} = t_{1d} = t_{2d} = C_a = C_d$	0
$i_{Ka} = i_{Kd}$	0
$i_{Ma} = i_{Md}$	0
$H_a = H_d$	0

In the application of SeismoStruct analysis, hysteretic curves were compared between lower and higher post-limit cyclic model parameters stiffness as shown in Figure 2.5. The ductility

of column web panel is measured based on the area of dissipating energy within the hysteretic loops. Initial elastic shear response followed by yielding and first lower bound gives similar results. As a result of this cyclic behaviour, near same cumulative rotation capacity for column web panel component is obtained for both tests. Lower post-limit stiffness of model parameter can be seen generated slightly greater area of dissipating energy. Theoretically, it is could be measured based on the degradation of the inclination curves which influences the hysteretic loops for every cycle after unloading path. It can be observed in Figure 2.5 that while the model parameter is increased by incrimination of post-limit stiffness, the amount of area in each cycle of loading is decreased.

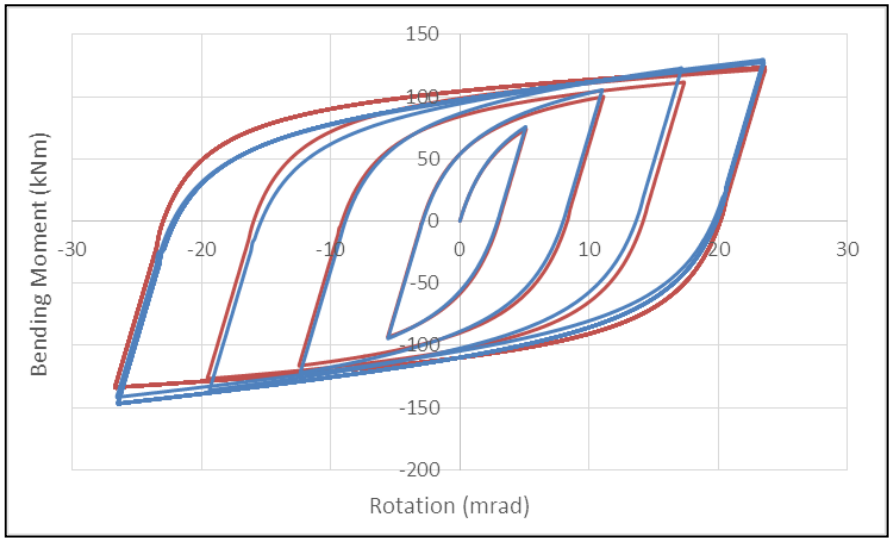

Figure 2.5 Comparison between Higher and Lower Post Limit Stiffness

2.3.3 End Plate, Column Flange and Flange Cleat

The components of column flange in bending and end-plate in bending generally are characterized by a bolted T-Stub behaviour with three different collapse mechanisms respectively as illustrated in Figure 2.6 and discussed in Eurocode 3. The characterization are devote in three parts which are plastic hinges form at the bolt-line and at the beam web under mode 1, plastic hinges form at the beam web followed by yielding of the bolts under mode 2 or yielding of the bolts only while the end-plate remains elastic under mode 3. Also presented in Eurocode 3, when all the components behaviour present in a bolt row are known, these values can be referred as springs connected in series.

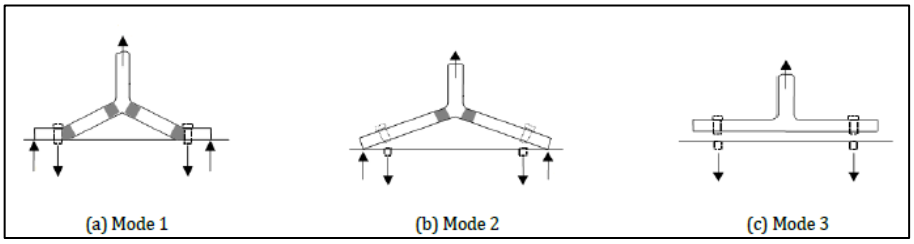

Figure 2.6 Failure Modes for a Bolted End-Plate Connections (Eurocode 3)

On the other hand, under the cyclic behaviour on the bolted connections can be strongly influenced by bolt plastic deformation. Excitation loads that produce inelastic deformations associated with dissipation of energy generate a moment-rotation response which is referred to as hysteresis. For this reason, the occurrence of such plastic mechanisms and deformations can lead to pinching effect of hysteresis loops of bolted components such as end-plate, column flange and flange cleat in bending.

To understand the pinching behaviour, lower and upper path are introduced, which represents moment-rotation values. Both upper and lower bounds regulate by Richard-Abbott type law, and are assigned by parameters Kop, Mop, Khp, np for lower bound curve and Ko, Mo, Kh, n for upper bound curve where the relevant parameters are defined as follows:

$$\begin{aligned} K_{ot} &= K_{op} + \left(K_o - K_{op}\right).t \\ M_{ot} &= M_{op} + \left(M_o - M_{op}\right).t \\ K_{ht} &= K_{hp} + \left(K_h - K_{hp}\right).t \\ n_t &= n_p + \left(n - n_p\right).t \end{aligned} \tag{2.1}$$

The parameter t, ranging in the interval [0,1], defines the transation law from the lower bound to the upper bound path and is given by:

$$t = \left[\frac{\left(\phi / \phi_{\lim}\right)^{t_1}}{\left(\phi / \phi_{\lim}\right)^{t_1} + 1} \right]^{t_2} \tag{2.2}$$

Where t_1, t_2 and $\phi_{\lim}$ are three experimentally calibrated parameters. Figure 2.7 shows, qualitatively, the resulting pinching behaviour with reference to one single excursion from the origin.

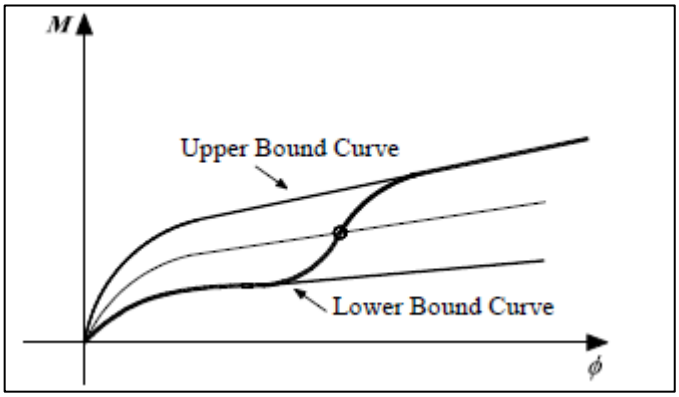

Figure 2.7 Loading Branch with Pinching

$$M = \frac{\left(K_{ot} + K_{ht}\right) x\phi}{\left[1 + \left|\frac{\left(K_{ot} + K_{ht}\right) x\phi}{M_{ot}}\right|^{n_t}\right]^{\frac{1}{n_t}}} + K_{ht}\, x\phi \qquad (2.3)$$

According to the experimental tests carried out by Nogueiro at al [13] the parameters in Table 2.3 can be observed which can be determined from eurocode 3 and experimental tests. The values for End-Plate in Bending are proposed in Table 2.4 which are subsequently used in SeismoStruct.

Table 2.3 Model Parameters for End-Plate in Bending

$K_a = K_d = K_{ap} = K_{dp}$ (KNm/rad)	EC3-1-8
$M_a = M_d = M_{ap} = M_{dp}$ (KNm)	EC3-1-8
$K_{pa} = K_{pd} = K_{pap} = K_{pdp}$ (KNm/rad)	
$n_a = n_d = n_{ap} = n_{dp}$	[1]
$t_{1a} = t_{1d}$	1
$t_{2a} = t_{2d}$	0
$C_a = C_d$	5
$i_{Ka} = i_{Kd}$	0
$i_{Ma} = i_{Md}$	0
$H_a = H_d$	0

Table 2.4 Example of Model Parameters for End-Plate in Bending

$K_a = K_d = K_{ap} = K_{dp}$ (KNm/rad)	4550
$M_a = M_d = M_{ap} = M_{dp}$ (KNm)	60
$K_{pa} = K_{pd} = K_{pap} = K_{pdp}$ (KNm/rad)	100
$n_a = n_d = n_{ap} = n_{dp}$	1
$t_{1a} = t_{1d}$	20
$t_{2a} = t_{2d}$	0.3
$C_a = C_d$	1
$i_{Ka} = i_{Kd}$	0
$i_{Ma} = i_{Md}$	0
$H_a = H_d$	0

The corresponding hysteretic curves can be observed in Figure 2.8. Hysteresis diagrams of joint panel component for pinching effect tests are plotted. It can be seen that joint panel shows less bending moment due to pinching effect and the area of dissipating energy.

Three analysed tests are shown in Figure 2.8 (i), (ii) and (iii) in SeismoStruct tests based on assigned parameters related to pinching respectively. Because of their geometrical properties and assigned higher model parameters, Figure 2.8 (i) and (ii) were more ifluenced by pinching. For these three analytical study, no stiffness or strength degradation were observed as can be seen in Figure 2.8. In some cases, the repetition of loading accompanied by degradation of the structural response because of deterioration of its mechanical properties. Previous study stated that the local pinching effect at the semi-rigid joints someimes effects considerably on the global response of the frame, and then it shall be considered properly in the mathematical modeling. The inelastic behavior of bolted connections is definitely more complex compared to welded joints, simply because more components can be involved in the dissipation mechanism, such as the endplate, angles or tee stubs in bending (depending on the connection typology), the column flange in bending, the panel zone in shear, the column web in tension or compression.

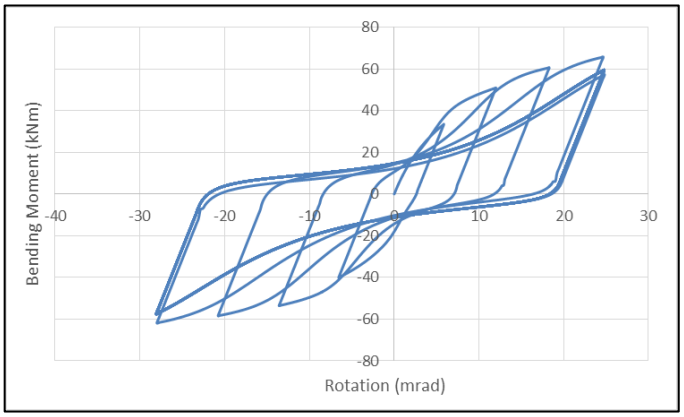

(i)

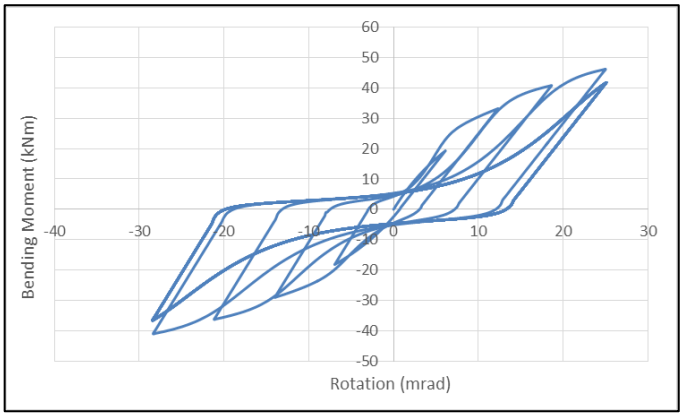

(ii)

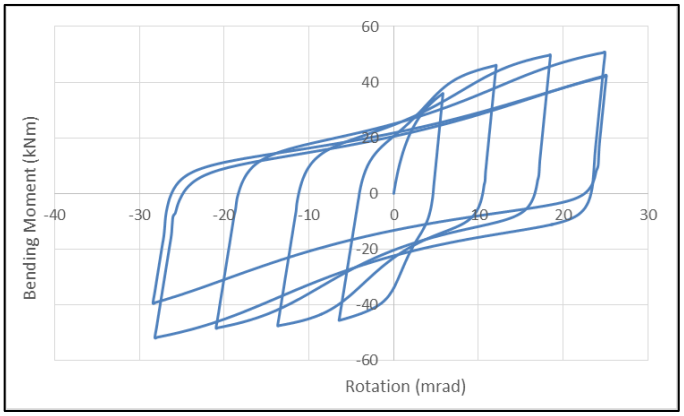

(iii)

Figure 2.8 Pinching Effects on the Joint

CHAPTER III: ANALYSIS OF COMPUTATIONAL RESULTS

3.1 Introduction

The necessity for additional investigation on analytical, experimental and numerical results regarding the behaviour of end-plate moment connections has been identified by the understanding of literature reviews. The analytical and numerical cyclic behaviour of double extended end-plate moment connections results is the main objective of this study.

The main purpose of the cyclic analysis was to investigate the strength, stiffness and inelastic rotational capacity of the connection assemblies and to determine and measure if extended end-plate moment connections were suitable for use in seismic force resisting moment frame. The development of a design procedure for end-plate moment connections subject to cyclic loading requires the study of analytical model that are able to simulate the moment-rotation response of the connection.

This chapter presents and compares the hysteretic moment-rotation curves of a connection tested experimentally with the analytical results when the Modified Richard-Abbott Model implemented in SeismoStruct is used and when the same parameters is implemented directly in a Spreadsheet. All computations were carried on using the methods described in Chapter II. The inputs correspond to the actual design parameters of the specimens tested experimentally by (Nogueiro, P., 2009) and are given in Figure 3.1.

3.2 Mechanical Model for Bolted Beam to Column Joints

The availability of methods in technical literature pertaining to the design modeling under cyclic behaviour of beam-column joints can be devoted into some groups which are mathematical models, mechanical models and finite elements models. Mathematical models like Modified Richard-Abbott Model are developed based on curve fitting of joint moment-rotation curves. However, mathematical approach can only be developed depending on the availability of experimental data and tests. On the numerical implementation and experimental calibration, it was observed that the controlling variable is rotation φ for this type of models.

Figure 3.2 (M. Latour, V. Piluso & G. Rizzano, 2011) illustrates a typical component model for an external double end-plate beam to column joint. Brittle components such as the bolts in tension can be identified and ductile components such as the column web panel in shear. The implementation of the mechanical model requires three steps to perform:

i) Assembling of the joint components;

ii) Modelling joint design parameters of the cyclic behaviour based Modified Richard-Abbott Model;

iii) Analysis and evaluation of joint cyclic moment-rotation capacity hysteretic loops.

The modified Richard-Abbott constitutes a sophisticated model and is used here to reproduce the cyclic behaviour of the steel joints.

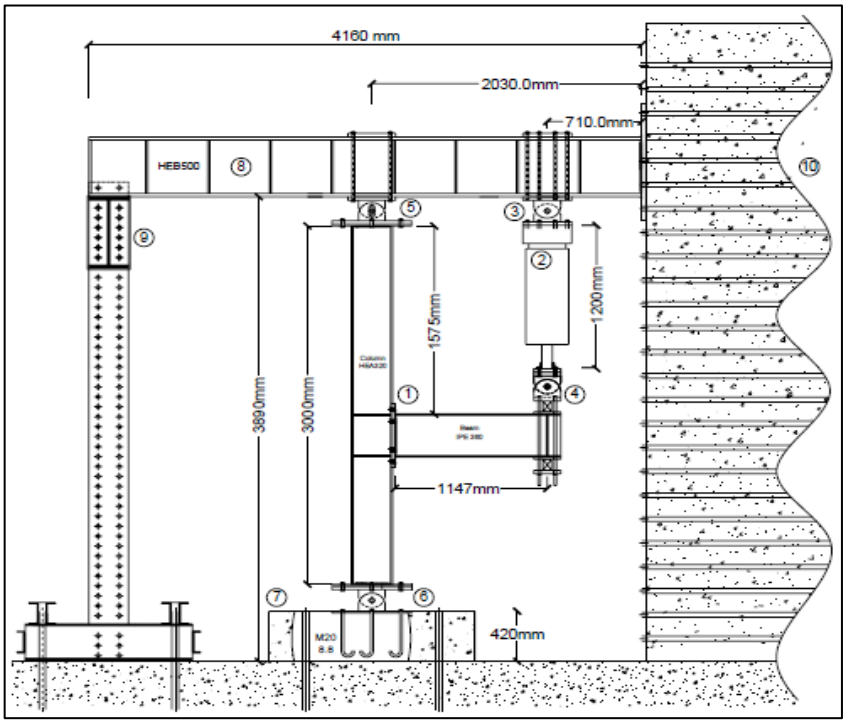

Figure 3.1 Load Scheme on Experimental Test (Nogueiro, P., 2009)

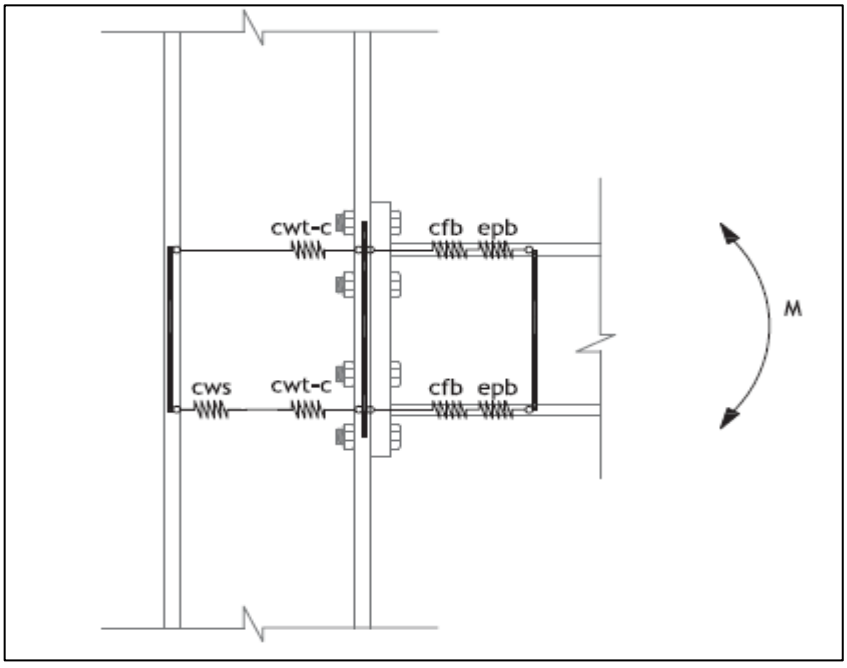

Figure 3.2 Mechanical Model for Bolted Extended End-Plate Connections (M. Latour, V. Piluso & G. Rizzano, 2011)

3.3 Double Extended End-Plate Bolted Connection

3.3.1 Model Analysis

The latest version of software Seismostruct is used for the analysis of the connection. SeismoStruct is a Finite Element package which capable of predicting the large displacement behaviour of space frames under static and dynamic loading. The software also takes into accounts both geometric non-linearities and material inelasticity. The analysed model consists on the link between a cantilever and a column, where the link element follows a moment-rotation law specified by the Modified Richard-Abbott model. The cyclic loading is applied on the extremity of the cantilever in order to produce a statically determined bending moment in the link. The rotation is obtained directly from the software in the link element.

In the analysis types, static time-history has been adopted during the analysis of these models. In static time-history analysis, the applied loads for example displacement, forces or a combination of both can vary independently in the pseudo-time domain which according to a prescribed load pattern. This type of analysis is typically used to model static of structures under various force or displacement patterns such as cyclic loading.

Bilinear steel model (stl_bl) was used for the beam and column elements. Five model calibrating parameters must be defined in order to fully describe the mechanical characteristics of the material as shown below in Table 3.1.

Table 3.1 Material Properties Beam and Column

Modulus of Elasticity, E (kPa)	2.10x10^8
Yield Strength, f_y (kPa)	450x10^3
Strain hardening parameter, μ	0.005
Fracture/buckling strain, ε_{ult}	0.1
Specific weight, γ (kN/m^3)	7.7

The joint modelled consists of a column section HEA 320 and a single beam section IPE 360 as illustrated in Figure 3.3. The geometry of the joint topology is presented in Figure 3.4 (Nogueiro, P., 2009).

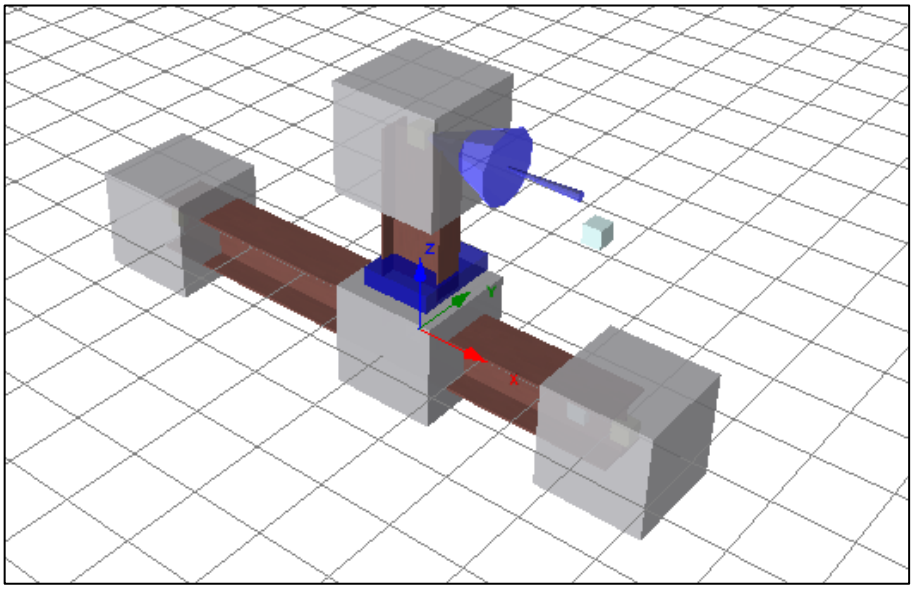

Figure 3.3 Geometry of Model Scheme in Seismostruct

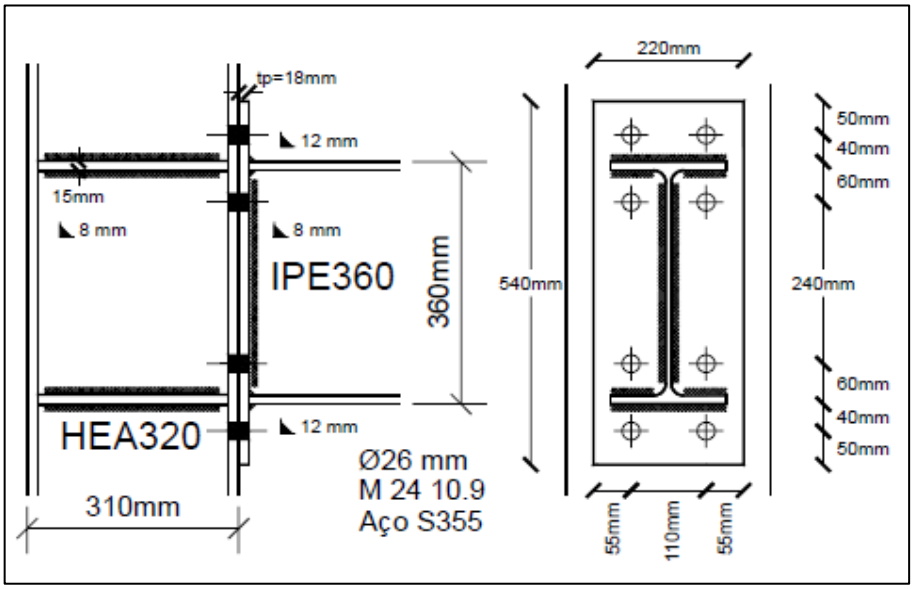

Figure 3.4 Geometry of Joint Topology

Element class are defining the element between classes and they are able to present nodes of beam, column and link element like joint. It is also allowing the modelling of different boundary conditions such as flexible foundations, seismic isolation, structural gapping/pounding and so forth. Link elements represent the connection of beam to column nodes. Its connect two initially coincide structural nodes and require the definition of an

independent force-displacement (or moment-rotation) response curve for each its local six degrees of freedom (F_1,F_2,F_3,M_1,M_2,M_3). In this analysis, only M_2 is interested and implemented by several definitions of Modified Richard-Abbott with thirty parameters as specified in Table 3.3

The ideal number of section fibres used in equilibrium computations assigned at each of the element´s integration sections is defined as shown in Table 3.2. The section fibres are to guarantee an adequate reproduction of the stress-strain distribution across the element´s model cross-section as illustrated in Figure 3.5.

Table 3.2 Discretization parameters

Section	Integration Section	Section Fibres
IPE 360	5	200
HEA 320	10	200

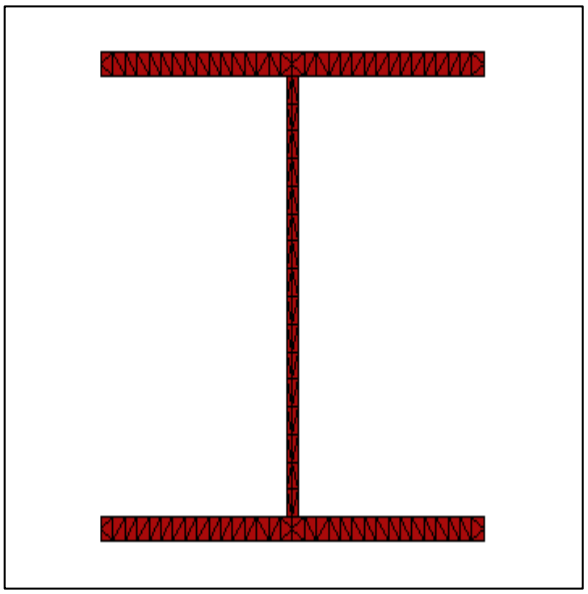

Figure 3.5 Section Discretization Pattern

Table 3.3 Model parameters for Modified Richard-Abbott model

Parameter	Description
K_a (and K_d) or K_{ap} (and K_{dp})	Initial stiffness for the upper or lower bound curve
M_a (and M_d) or M_{ap} (and M_{dp})	Strength for the upper or lower bound curve
K_{pa} (and K_{pd}) or K_{pap} (and K_{pdp})	Post limit elastic stiffness for the upper or lower bound curve
n_a (and n_d) or n_{ap} (and n_{dp})	Shape parameter for the upper or lower bound curve
t_{1a} and t_{1d}	Empirical parameters related to pinching
t_{2a} and t_{2d}	Empirical parameters related to pinching
C_a and C_d	Calibration parameters related to pinching
i_{Ka} and i_{Kd}	Empirical parameters related to the stiffness damage rate
i_{Ma} and i_{Md}	Empirical parameters related to the strength damage rate
H_a and H_d	Empirical coefficient defining the level of isotropic hardening
E_{maxa} (and E_{maxd})	Maximum value of deformation reached in the loading history

The model must be experienced loading and unloading branches which can be either large or small according to load protocol. To illustrate and validate the model parameter, the numerical analyses were compared with the real experimental test. The joint was assigned with its properties defined in Table 3.4 considering stiffness and strength damage rate.

Table 3.4 Model Parameters for Joints J1-3

$K_a = K_d = K_{ap} = K_{dp}$ (KNm/rad)	55600
$M_a = M_d = M_{ap} = M_{dp}$ (KNm)	285
$K_{pa} = K_{pd} = K_{pap} = K_{pdp}$ (KNm/rad)	5500
$n_a = n_d = n_{ap} = n_{dp}$	1
$t_{1a} = t_{1d}$	1
$t_{2a} = t_{2d}$	1
$C_a = C_d$	0.00001
$i_{Ka} = i_{Kd}$	0.5
$i_{Ma} = i_{Md}$	0.0001
$H_a = H_d$	0.00001
E_{maxa} (rad)	0.1

Time-history load curve is shown in Figure 3.6. The calibration of load protocol is followed by experimental test (Nogueiro, P., 2009) which was based on ECCS loading protocol. Due to the test limitation course of actuator (load application system), the cyclic load amplitude remain uniform until its reach failure of the joint. The time-history load curve data is listed in appendix A.

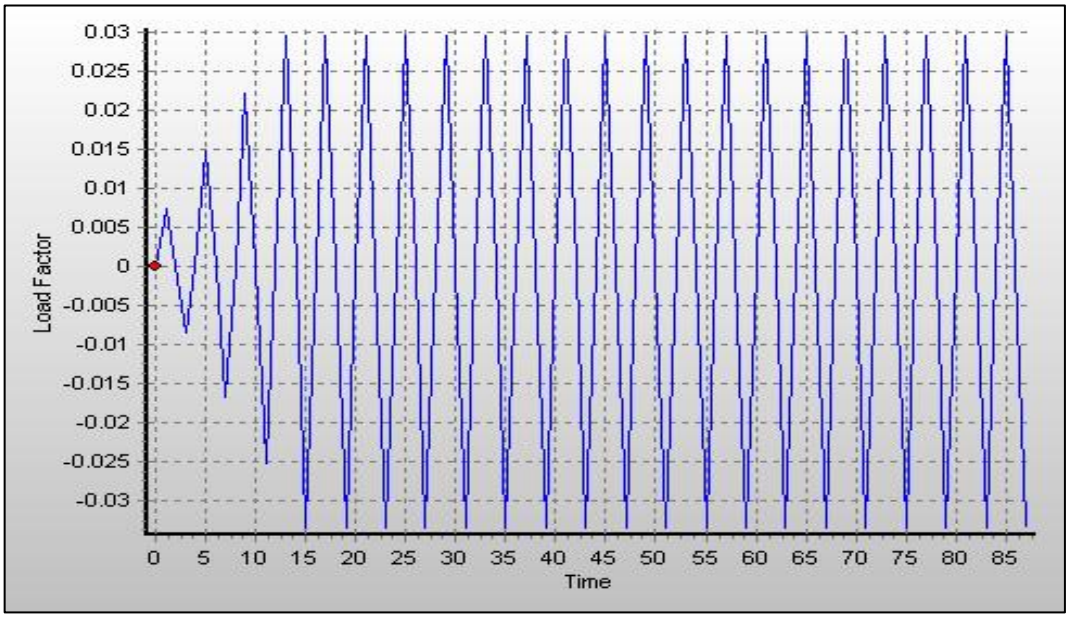

Figure 3.6 Time-History Load Curve

3.3.2 Comparison of Experimental and SeismoStruct Analysis

In this section, relevant information from experimental test (Nogueiro, P., 2009) that is pertinent to the analysis made is presented to validate the analytical approach. This was undertaken to facilitate the discussion of results and to highlight some comparative aspects of the cyclic behaviour. All analysis presented in this section were evaluation of extended end-plate moment connections. The experimental test of cyclic curves presented in Figure 3.7.

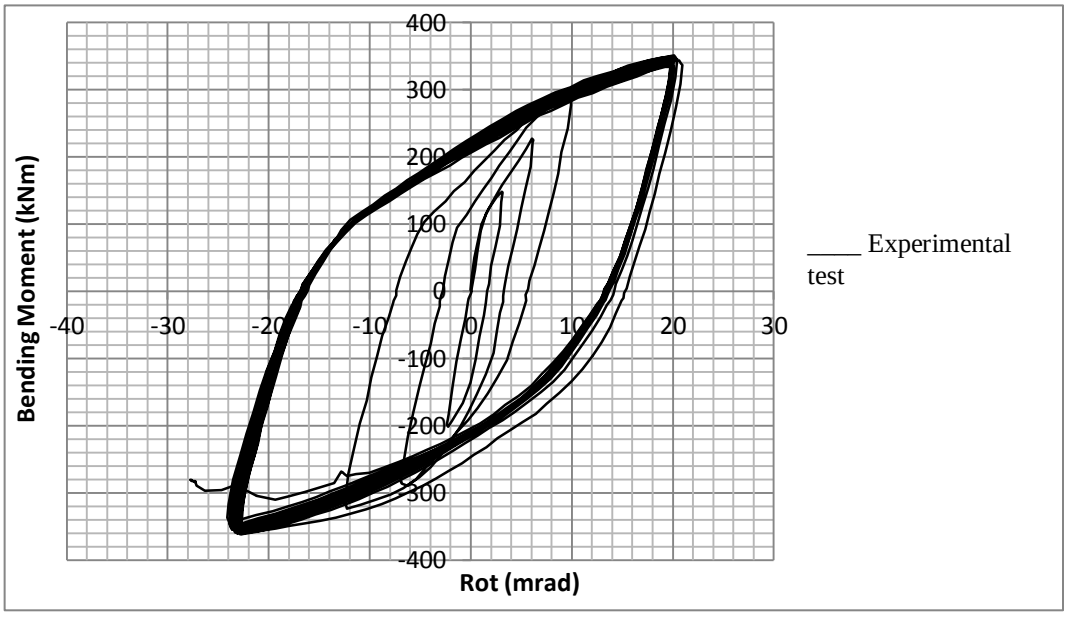

Figure 3.7 Experimental Moment-Rotation Curve

The result of the analytical analysis is shown in Figure 3.8. Theoretically, hysteretic curves comprising upper and lower bounds which represents loading and unloading load paths while the prediction of moment resistance and the stiffness of the connection are related to the size of the connected members, types of joints and orientation of the column axis.

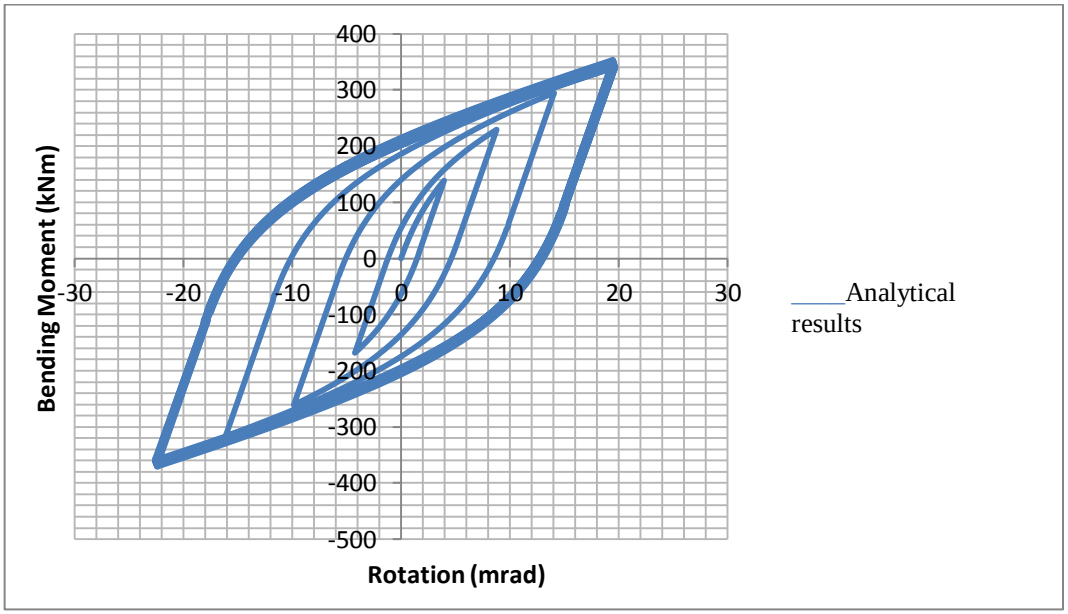

Figure 3.8 Numerical Moment-Rotation Curve

By inspection of the diagrams in Figure 3.9, it can be seen that the experimental and analytical cyclic curves behave in similar pattern and match with each other in their last cyclic curve lines. The comparison validates analytical results and corresponding results can be used to implement in numerical approach. In addition, the cyclic load pattern gives very good prediction for the energy dissipation capacity of the analysed connections.

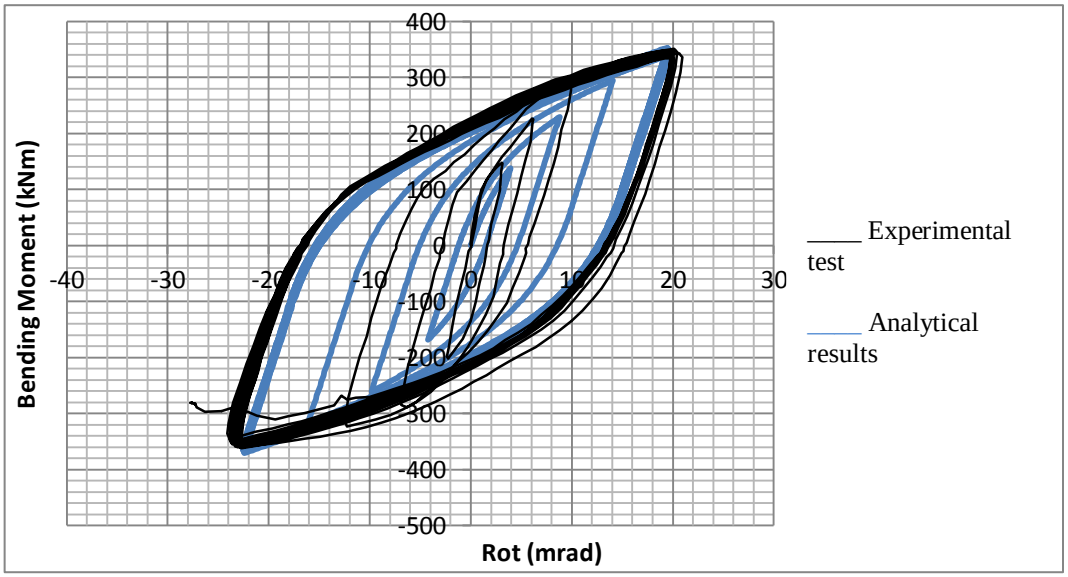

Figure 3.9 Comparison between Experimental and Numerical Moment-Rotation Curve

3.3.3 Numerical Study Based on Modified Richard-Abbott Model

The first branch stiffness is identical to the initial stiffness of a non-linear behaviour and it is defined in Modified Richard-Abbott as the following formula (Nogueiro, P., 2009):

$$M = \frac{\left(k - k_p\right).\phi}{\left[1 + \left|\frac{\left(k - k_p\right).\phi}{M_0}\right|^N\right]^{1/N}} - k_p.\phi \tag{3.1}$$

$$N = \frac{-\ln 2}{\ln\left(\frac{M_1}{M_0} - \frac{k_p}{k - k_p}\right)} \tag{3.2}$$

With the application of formula aforementioned above, Figure 3.10 shows the initial stiffness of moment-rotation curve. Its can be observed that joint behave in a ductile manner while experiencing the loading. Yield point was observed of the connection of approximately 116.90 kN.m. Table 3.5 shown the data inclination of bending moment-rotation at the joint.

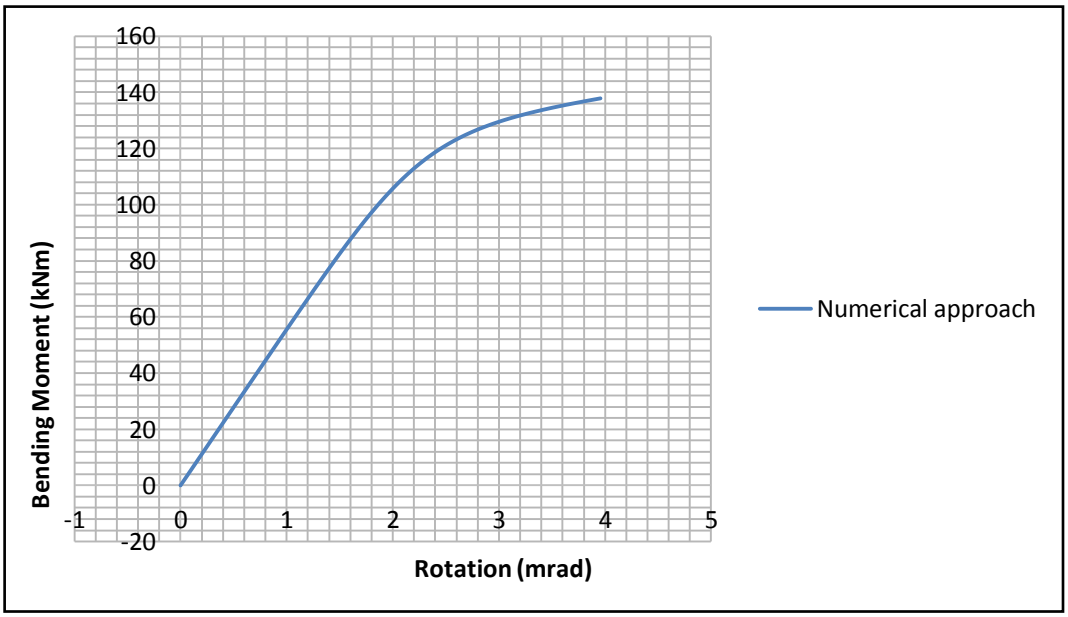

Figure 3.10 Intial Stiffness Numerical Moment-Rotation Curve

Table 3.5 Initial Stiffness Numerical Data

Time Step, dt	Rotation, ϕ	Numerical Moment
0	-0.000364999	-0.020293954
0.01	-0.000365038	-0.020296116
0.2	0.64843	36.05006878
0.4	1.39369	76.96057011
0.6	2.19779	112.819075
0.8	3.05442	130.1644829
1.0	3.95691	137.8419371

Figure 3.11 shows the second part of unloading path. In this test of asymmetrical joints with respect to centroidal axis, the models were verified based on formula 3.3. The numerical results are given in Table 3.6. In terms of maximum bending moment of upper and lower bound, both exhibited stable hysteretic behaviour with approximately 137.842 kNm and 158.82 kN.m on the lower and upper bound curve respectively. The corresponding values for rotation are 3.957 mrad and -4.2398 mrad respectively.

$$M = M_n - \frac{\left(k_a - k_{pa}\right).\left(\phi_n - \phi\right)}{\left[1 + \left|\frac{\left(k_a - k_{pa}\right).\left(\phi_n - \phi\right)}{M_{oa}}\right|^N\right]^{1/N}} - k_{pa}.\left(\phi_n - \phi\right) \tag{3.3}$$

Where:

M_0 is Reference Bending Moment

N is Parameter Adjustment

M_n is Negative bending moment, a link at the end of descending half cycle

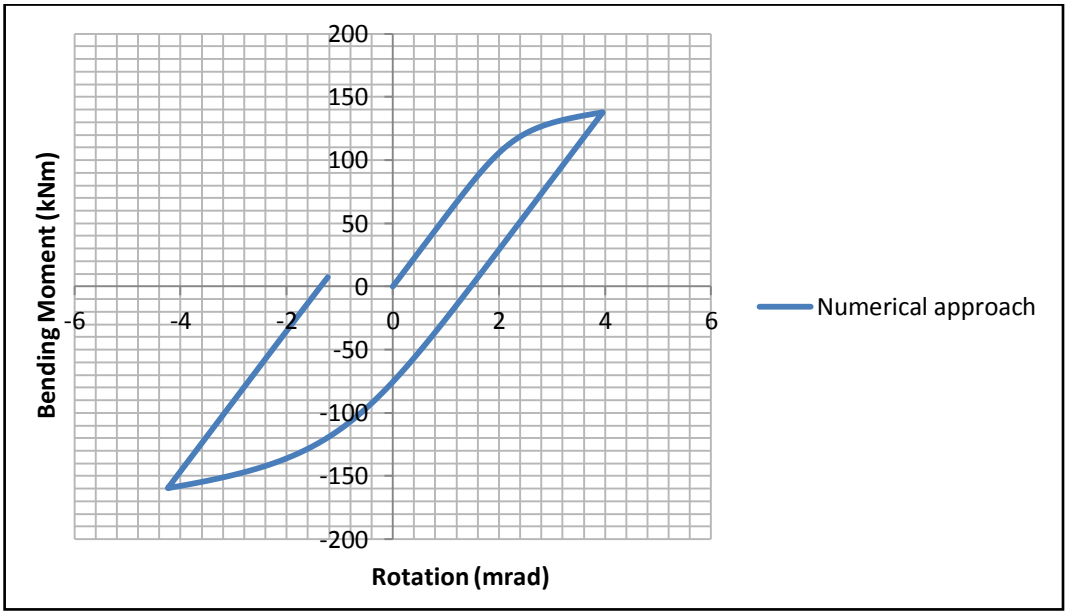

Figure 3.11 Lower and Upper Numerical Moment-Rotation Curve

Table 3.6 Lower and Upper Numerical Data

Time Step, dt	Rotation, ϕ	Numerical Moment
1.0	3.95691	137.8419371
1.5	2.34458	48.21068312
2.0	0.67799	-42.531561
2.5	-1.60788	-128.5884013
3.0	-4.2399	-159.58241

The complete curve in the Figure 3.12 is calculated in the same formula by replacing (M_n, ϕ_n) by (M_p, ϕ_p) and the parameters M_{0a}, k_a and k_{pa} by the corresponding values evaluated at unloading, M_{0d}, k_d and k_{pd}. The semi-rigid joint exhibited adequate stable hysteretic behaviour with large ductility levels. The test was terminated at a displacement 19.61559 . Table 3.7 shows the cyclic data including upper and lower bound curve of the numerical approach.

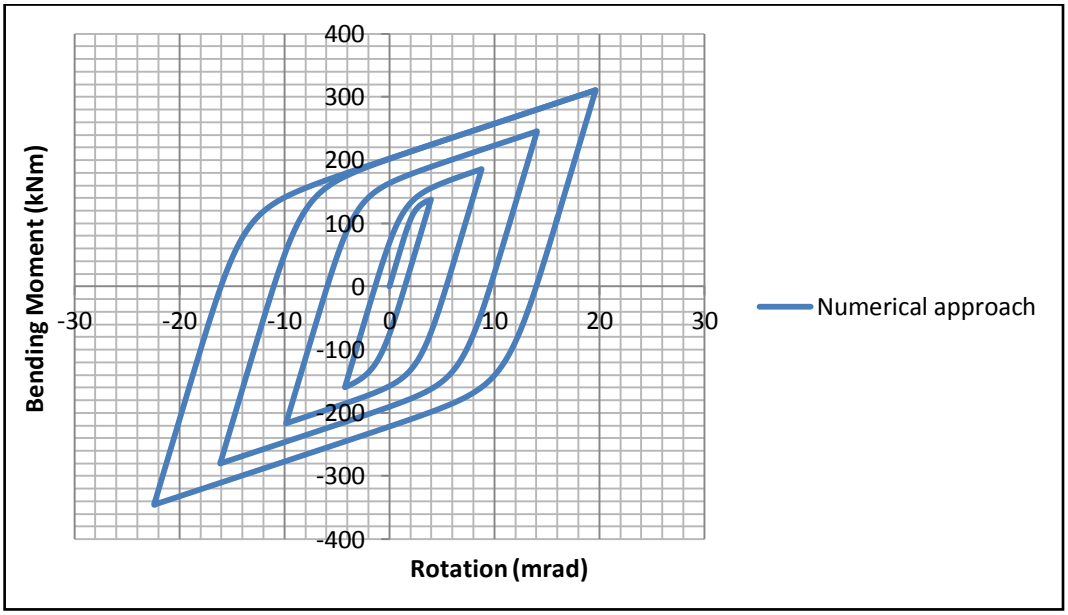

Figure 3.12 Complete Numerical Moment-Rotation Curves

Table 3.7 Complete Numerical Curves Data

Time Step, dt	Rotation, ϕ	Numerical Moment
1.0	3.95691	137.8419371
2.0	0.67799	-42.531561
4.0	-0.56173	42.17209655
6.0	1.75529	-136.8833392
8.0	-1.85219	143.0853446
10	2.53413	-174.071674
12	-2.76341	184.829574
14	3.16423	-203.4349711
16	-3.19526	184.6653086
17	19.61559	310.6611397

3.3.4 Comparison of SeismoStruct Analysis and Analytical Implementation of Model

On the basis of this verification it can be stated that the joint gives good prediction for the initial part of the moment-rotation curve, the moment capacity. However, it is very obvious that the yielding point slightly differ while experiencing loads as shown in Figure 3.13. The gaps between the values are probably due to the analysis implementation done in SeismoStruct that could be differed from numerical approach and the geometrical model itself. The comparison between analytical and numerical initial stiffness data is shown in Table 3.8.

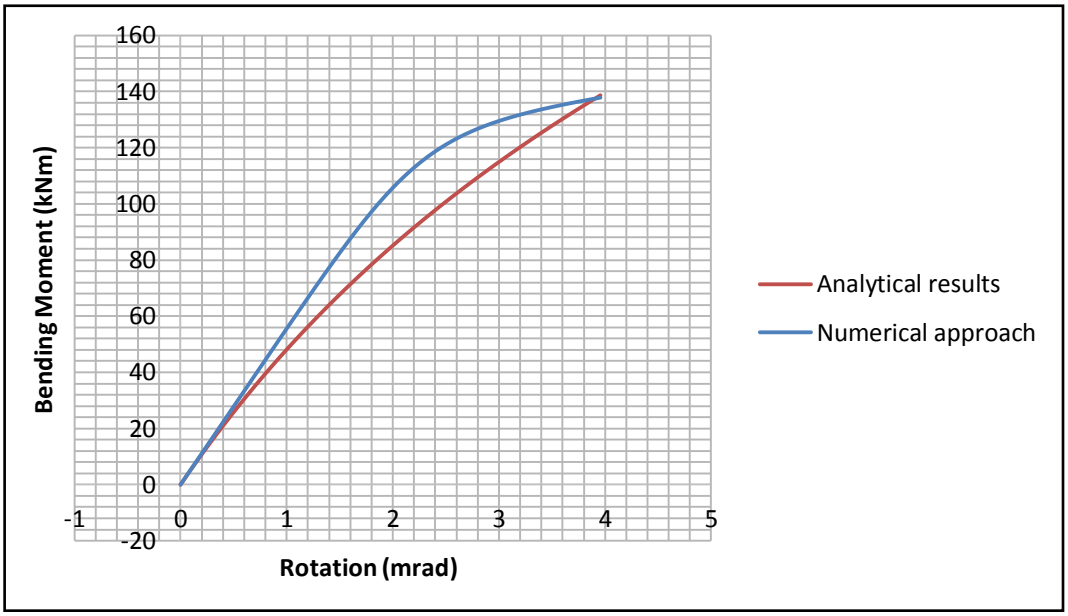

Figure 3.13 Comparison between Analytical and Numerical Initial Curve

Table 3.8 Comparison between Analytical and Numerical Initial Stiffness Data

Time Step, dt	Rotation, ϕ	Numerical	Analytical	% Error
0	-0.000364999	-0.020293954	-0.02031851	-0.121001555
0.01	-0.000365038	-0.020296116	-0.02037163	-0.372061334
0.2	0.64843	36.05006878	32.72908324	9.212147584
0.4	1.39369	76.96057011	63.7501562	17.16517158
0.6	2.19779	112.819075	91.51311104	18.88507237
0.8	3.05442	130.1644829	116.3666166	10.60033121
1.0	3.95691	137.8419371	138.6804326	-0.608302174

The unloading curve for the first branch experienced almost similar results before reach to the second part of post-limit stiffness as shown in Figure 3.14. Its means that the zone model gives very good prediction for the unloading stiffness of the analysed connections. The second lower bound shows the similar cyclic behaviour as in the initial rotational stiffness. Its behaviour must be influenced by the interaction of earlier cycle and generate a reversal moment-rotation pattern. While the joint is preceded by loading, the ascending behaviour results the similar pattern on the curve line. This is also due to the interaction of the descending pattern at the first branch. Simply said that the initial stiffness of the connection is very similar at the beginning but became slightly in gap after proceeding to yielding point. The phenomena curve pattern can judge on the beam-column connection and joint geometrical topology on both type of implementation.

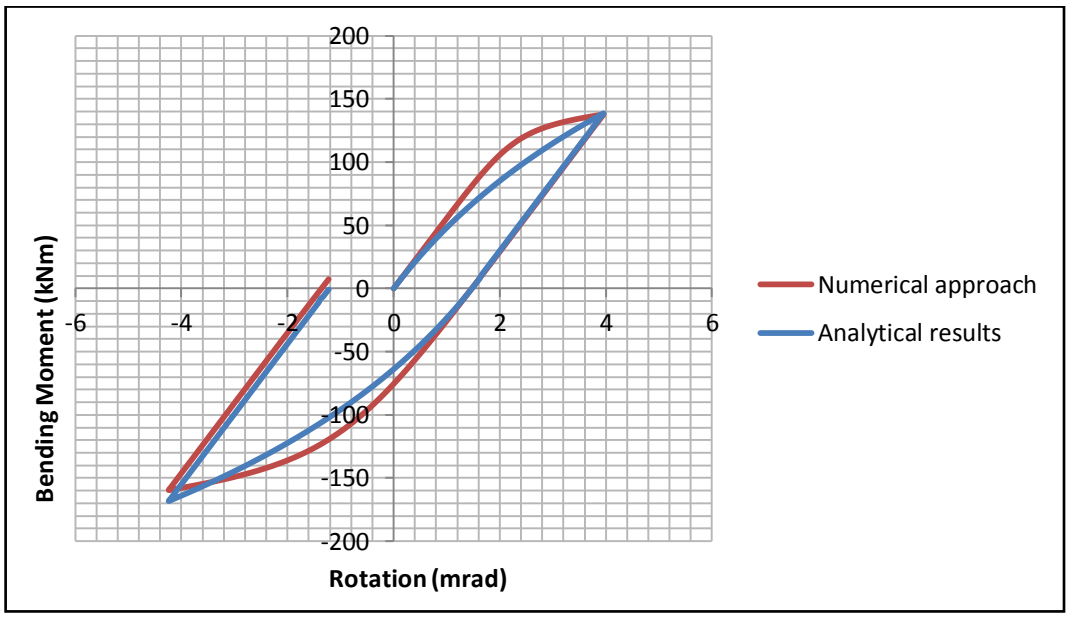

Figure 3.14 Comparison between Analytical and Numerical of Lower and Upper Curve

Table 3.9 Comparison between Analytical and Numerical of Lower and Upper Data

Time Step, dt	Rotation, ϕ	Numerical	Analytical
1.0	3.95691	137.8419371	138.6804326
1.5	2.34458	48.21068312	49.03374664
2.0	0.67799	-42.531561	-37.59827671
2.5	-1.60788	-128.5884013	-112.5232063
3.0	-4.2399	-159.58241	-168.2731755

The complete comparison curves of cyclic behaviour can be seen in Figure 3.15. Numerical curves are slightly downward as compared to analytical analysis. However, the cyclic pattern connection displayed a great deal of ductility and energy dissipation capacity.

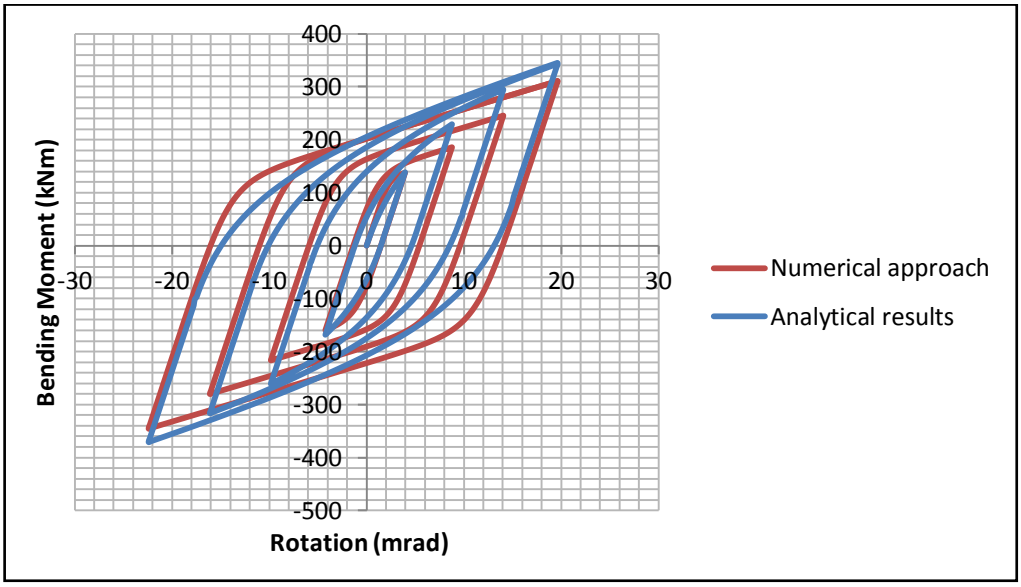

Figure 3.15 Complete comparison between analytical and numerical curve

Table 3.10 Complete Comparison between Analytical and Numerical Data

Time Step, dt	Rotation, ϕ	Numerical	Analytical
1.0	3.95691	137.8419371	138.6804326
2.0	0.67799	-42.531561	-37.59827671
4.0	-0.56173	42.17209655	31.07797965
6.0	1.75529	-136.8833392	-97.27326898
8.0	-1.85219	143.0853446	102.5689259
10	2.53413	-174.071674	-140.413437
12	-2.76341	184.829574	153.0530765
14	3.16423	-203.4349711	-175.3135119
16	-3.19526	184.6653086	176.979478
17	19.61559	310.6611397	345.1613924

3.3.5 Parameter Sensitivity by Applying Solver Approach

In this section, the sensitivity of certain parameters is investigated by implementing spreadsheet solver. This is done by minimizing the sum of moment errors by changing the input parameters in Modified Richard-Abbott model in order to find the similar results and matching the cyclic curves. In this case, initial stiffness (Ka and Kd) and post limit elastic stiffness (Kpa and Kpd) are involved. The percentages of error were calculated to find the differences between analytical and solver approach. The results were analysed and discussed whether this approach can be used to fit the curves. The Figure 3.16 shows the initial ascending curve resulted by solver analysis.

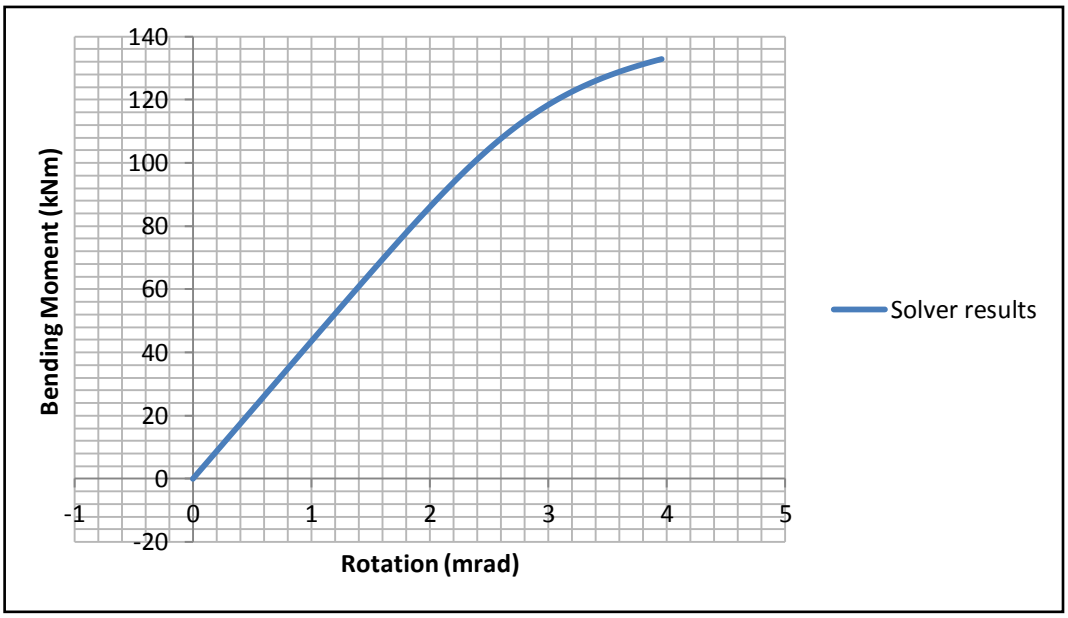

Figure 3.16 Initial Stiffness Solver Moment-Rotation Curve

Figure 3.17 shows the comparison of three results by analytical, numerical and solver analysis. The data are tabulated in Table 3.11. It shows a good and closer values between analytical and solver analysis. The parameters, Ka and Kd are reduced to 43549.05 kNm/rad and Kpa and Kpd are aslo reduced to 4940.33 kNm/rad from original parameters.

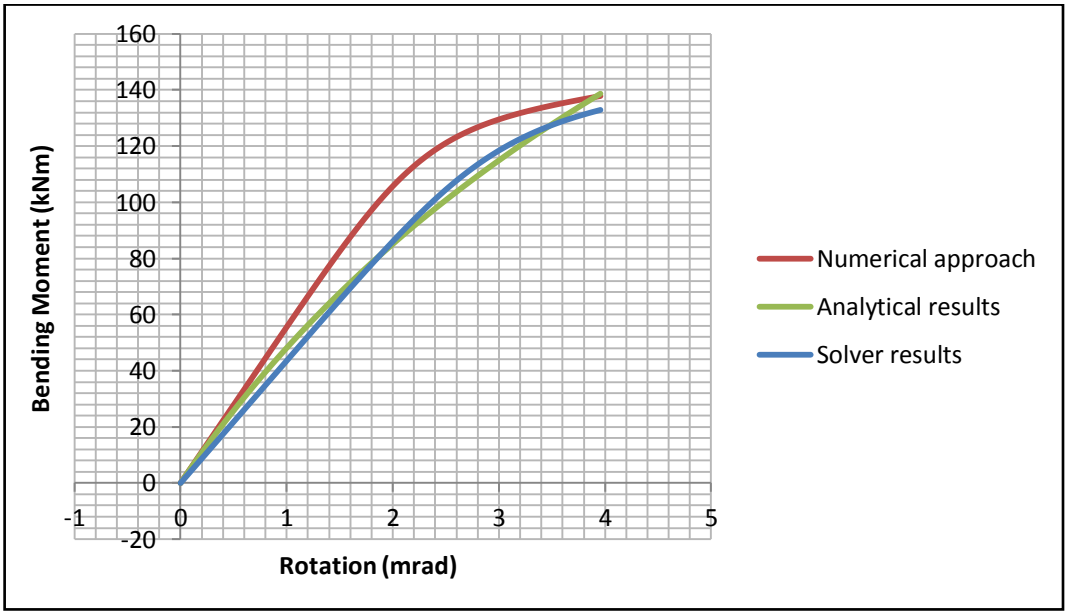

Figure 3.17 Comparison of Initial Stiffness by Analytical, Numerical and Solver Moment-Rotation Curves

Table 3.11 Comparison of Initial Stiffness by Analytical, Numerical and Solver Data

Time Step, dt	Rotation, ϕ	Numerical	Analytical	Solver	% Error
0	-0.000364999	-0.020293954	-0.02031851	-0.015895366	21.7690372
0.01	-0.000365038	-0.020296116	-0.02037163	-0.015897059	21.9647176
0.2	0.64843	36.05006878	32.72908324	28.23807762	13.72175807
0.4	1.39369	76.96057011	63.7501562	60.6058559	4.93222368
0.6	2.19779	112.819075	91.51311104	93.76797458	-2.463978674
0.8	3.05442	130.1644829	116.3666166	119.6069647	-2.784602831
1.0	3.95691	137.8419371	138.6804326	132.8818339	4.181266666

Figure 3.18 shows the loading and unloading by analytical, numerical and solver moment-rotation curves. The unloading part gives a match curve lines with less percentage of errors

between analytical and solver analysis. The second part of descending also shows a similar pattern between these two curves. On the other hand, the initial stiffness, Ka and Kd is increased to 51885.07 kNm/rad and post-limit stiffness, Kpa and Kpd is decreased to 4918.30 kNm/rad as compared to the first curve. However, both branches reduced the initial and post stiffness parameters from the original inputs.

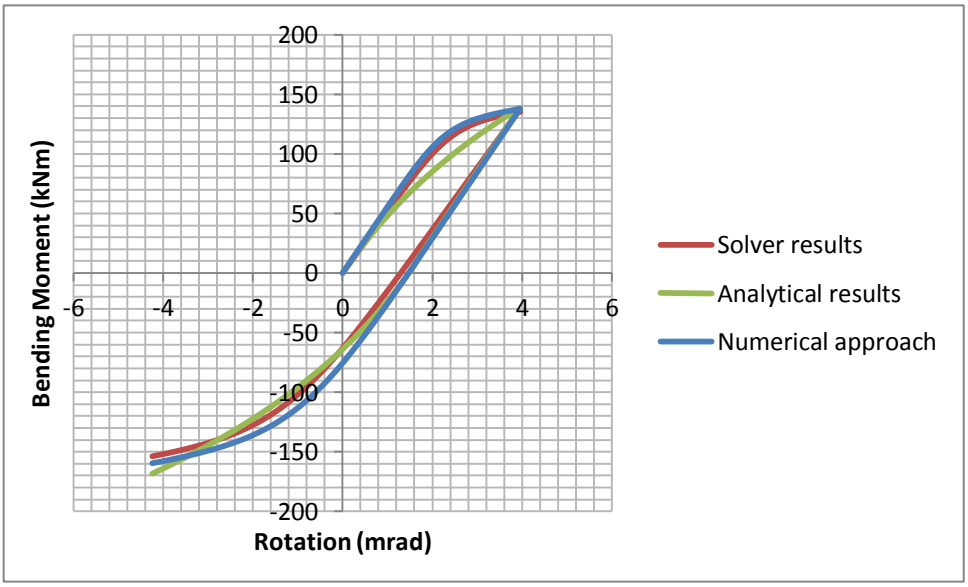

Figure 3.18 Comparison of Loading and Unloading by Analytical, Numerical and Solver Moment-Rotation Curves

Table 3.12 Comparison of Loading and Unloading by Analytical, Numerical and Solver Data

Time Step, dt	Rotation, ϕ	Numerical	Analytical	Solver	% Error
1.0	3.95691	137.8419371	138.6804326	135.1679921	2.53275854
1.5	2.34458	48.21068312	49.03374664	54.19516582	-10.52625902
2.0	0.67799	-42.531561	-37.59827671	-31.03493414	17.45649839
2.5	-1.60788	-128.5884013	-112.5232063	-119.1184262	-5.861208649
3.0	-4.2399	-159.58241	-168.2731755	-153.739657	8.636859949

CHAPTER IV: CONCLUSIONS AND RECOMMENDATIONS

4.1 Conclusions

Based on the analytical and numerical investigation conducted on the bolted beam to column connection the latter conclusions are discussed. The mechanical component ductility cannot be denied that plays an important role as to sustain the strength of connection. The column flange and the end plate in bending and the column web panel in shear are ductile joint components. Therefore, the bolts in tension and shear and welds are typical examples of brittle components. Thus, both types mode of failure should not interfere the strength of the connection. It is also suggest that the experimental model should be avoided with any distortion and damage due to site work which can cause certain gaps in results.

A component method design philosophy is taken directly from Eurocode 3 with strength checks on steel, weld and bolts which are assemble to integrate as a one bolted joint. The accurate calculation and observation should be made on joint behaviour when assembled either react as individual component or behave in one structure. Indeed, there are many consideration and analytical procedures on determination of joint response particularly beyond the elastic limit of the moment-rotation curve. The cyclic behaviour of beam to column joint plays an important aspect of a steel moment resisting framed structure especially under seismic excitation.

The analytical results and numerical implementation demonstrated that the joints beam-column connection is able to dissipate certain amount of energy capacity to withstand inelastic deformations resulting from seismic forces. The numerical procedure which based on Modified Richard-Abbott Model was developed in spreadsheet and presented in this dissertation. SeismoStruct analyse the model by implementing stress-strain curve which based on fibre model while Modified Richard-Abbott Model correlate with moment-rotation curve. This could be the major reason differences between results since both implement and analysing different approach. It is evident that initial and post-limit stiffness behaviour results in different curvature as compared between analytical and numerical results.

The implementation of solver analysis when compared to analytical results does influence the curvature lines. It can be said that in order to achieve similar curves between analytical and solver analysis, certain amount of initial and post stiffness parameters should be reduced that lead to match results. However, this theory is still weak since more analysis should be done to improve the results.

The conclusion is that the relation of the components characteristics of the structure in respect to the parameters model under seismic loads has major influences during the analysis of the seismic resistance of the structure. It is obvious that the joint characteristic, that is the geometrical and material properties, may have significant influence on the moment-rotation behaviour of the joint.

4.2 Recommendations

There are still open questions in the field of beam to column extended end-plate connections. On the basis of the research presented in this dissertation the following recommendations can be given for further work:

i) Beam-Column joints assemblages in this study were designed according to model parameters. In order to precisely getting the same results design and structure modelling during experimental and software illustration must fit into each other without any distortion and damage on the model during experimental tests.

ii) Due to the error or gap in the result, analytical procedures should be investigated onto the numerical implementation. It is suggested to observed the root of the Modified Richard-Abbott Model which certainly derive from stress-strain which based on fibre analysis and correlating with moment-rotation numerical form.

REFERENCES

Ádány S., "Numerical and Experimental Analysis of Bolted End-Plate Joints under Monotonic and Cyclic Loading", PhD thesis presented to the Budapest University of Technology and Economics, (2000).

Ashraf, M. G. (1991). "Extended End-Plate Beam-Column Joints in Seismic Moment Resisting Frames," Degree Doctor of Philosophy Thesis, MacMaster University, Hamilton, Ontario.

Beg M., Zupancic E. and Vayas I. (2004) "On the Rotation Capacity of Moment Connections" Journal of Constructional Steel Research. 60, 601–620.

Boorse, M. R. (1999). "Evaluation of the Inelastic Rotation Capability of Flush End-Plate Moment Connections," Master of Science Thesis, Virginia Polytechnic Institute and State University, Blacksburg, Virginia.

Dunai D.Sc., (2011) "Type Testing of Buckling Restrained Braces according to EN 15129", Final Report, Department of Structural Engineering, Budapest University of Technology and Economics.

Elnashai, A.S. and Elghazouli, A.Y. (1994) "Seismic Behaviour of Semi-rigid Steel Frames" Journal of Constructional Steel Research. 29, 149-174.

Elnashai, A.S., Elghazouli, A.Y. and Denesh-Ashtiani. F. A. (1998) "Response of Semi-rigid Steel Frames to Cyclic and Earthquake Loads." Journal of Structural Engineering. 857-867.

Gerami M., Saberi H., Saberi V. and Saedi Daryan A. (2011) "Cyclic Behavior of Bolted Connections with Different Arrangement of Bolts" Journal of Constructional Steel Research. 67, 690–705.

Helena Gervásio., Simões da Silva, L. and Borges, L. (2004). Reliability Assessment of the Post-Limit Stiffness and Ductility of Steel Joints. Journal of Constructional Steel Research. 60, 635-648.

Kim, W. and Lu, W. (1992) “Hysteretic Analysis of Composite Beam-to-Column Joints” Earthquake Engineering, Tenth World Conference. 4541-4546.

Kumar, S. and Rao, D.V. (August 1-6, 2004). Seismic Qualification of Semi-Rigid Connections in Steel Frames. 13th World Conference on Earthquake EngineeringVancouver, B.C., Canada. Paper No. 2149.

Mahmood, T. and Azman, H. (2008). Experimental Tests on Extended End-Plate Connections with Variable Parameters. Steel Structures 8 (2008). 369-381.

Nogueiro, P., “Comportamento Cíclico de Ligações Metálicas”, PhD thesis presented to the University of Coimbra, (2009).

Nogueiro, P. Simões da Silva, L., Bento, R and Simões, R., “Numerical implementation and calibration of a hysteretic model with pinching for the cyclic response of steel joints”, International Journal of Advanced Steel Construction 3(1). Pp. 459-484 (2007).

Nogueiro, P. Simões da Silva, L., Bento, R and Simões, R.,“Experimental behaviour of standardised European end-plate beam-to-column steel joints under arbitrary cyclic loading”, in Camotim, D. (ed.), Proceedings of SDSS’06 International Colloquium on Stability and Ductility of Steel Structures, Lisboa, Portugal, 6-8 September (2006).

Ryan, J. C. (1999). “Evaluation of Extended End-Plate Moment Connections Under Seismic Loading,” Master of Science Thesis, Virginia Polytechnic Institute and State University, Blacksburg, Virginia.

Saqan, E. I. (December 1995). “Evaluation o Ductile Beam-Column Connections for use in Seismic-Resistant Precast Frames,” Doctor of Philosophy Dissertation, The University of Texas at Austin.

SeismoSoft (2011). SeismoStruct Version 5.2.2. SeismoSoft Ltd., Inc., Earthquake Engineering Software Solutions, Pavia, Italy, [online]. Available from URL: http://www.seismosoft.com.

Setia, S., Murty, C.V.R. and Sehgal V.K. (2008). Improved Configuration of Weak-Axis Connections in Seismic Steel Moment Frames. The 14th World Conference on Earthquake Engineering October 12-17, 2008, Beijing, China.

Shemy, S.B. and Sreekumar, S. (Sep-Oct. 2012) “A Ductility Model for Steel Connections.” International Journal of Modern Engineering Research (IJMER). Vol.2, Issue.5, pp-3517-3521. ISSN: 2249-6645.

Simões da Silva, L. and Girão Coelho A. (2001) “A Ductility Model for Steel Connections.” Journal of Constructional Steel Research. 57, 45–70.

Simões da Silva, L., Rebelo, C., and Mota, L., (2009) “Extension of the Component Method to End-Plate Beam-to-Column Steel Joints Subjected to Seismic Loading” CC2009 – Special Lecture, Madeira.

Steenhuis, M., Jaspart, J. P., Gomes, F. and Leino, T. (1998). Application of the Component Method to Steel Joints, Proceedings of the Control of the Semi-Rigid Behaviour of Civil Engineering Structural Connections Conference, ed. by R. Maquoi, COST C1, Liege, Belgium. 125-143.

Sokol Z., Wald F., Delabre V., Muzeau J. P and Marek S. “Design of End Plate Joints Subject to Moment and Normal Force”. Czech Technical University in Prague, Université Blaise Pascal, CUST.

Yorgun, C. (2001) “Evaluation of Innovative Extended End-Plate Moment Connections under Cyclic Loading”. Department of Civil Engineering, Istanbul Technical University. 483-492.

APPENDIX A

Time-history curve values

Time	Load Factor
0.01	0.
1.	0.00741061
2.	0.
3.	-0.00834668
4.	0.
5.	0.01482121
6.	0.
7.	-0.01669337
8.	0.
9.	0.02223182
10.	0.
11.	-0.02504005
12.	0.
13.	0.02964243
14.	0.
15.	-0.03338673
16.	0.
17.	0.02964243

18.	0.
19.	-0.03338673
20.	0.
21.	0.02964243
22.	0.
23.	-0.03338673
24.	0.
25.	0.02964243
26.	0.
27.	-0.03338673
28.	0.
29.	0.02964243
30.	0.
31.	-0.03338673
32.	0.
33.	0.02964243
34.	0.
35.	-0.03338673
36.	0.
37.	0.02964243
38.	0.
39.	-0.03338673
40.	0.
41.	0.02964243
42.	0.

43.	-0.03338673
44.	0.
45.	0.02964243
46.	0.
47.	-0.03338673
48.	0.
49.	0.02964243
50.	0.
51.	-0.03338673
52.	0.
53.	0.02964243
54.	0.
55.	-0.03338673
56.	0.
57.	0.02964243
58.	0.
59.	-0.03338673
60.	0.
61.	0.02964243
62.	0.
63.	-0.03338673
64.	0.
65.	0.02964243
66.	0.
67.	-0.03338673

68.	0.
69.	0.02964243
70.	0.
71.	-0.03338673
72.	0.
73.	0.02964243
74.	0.
75.	-0.03338673
76.	0.
77.	0.02964243
78.	0.
79.	-0.03338673
80.	0.
81.	0.02964243
82.	0.
83.	-0.03338673
84.	0.
85.	0.02964243
86.	0.
87.	-0.03338673